

# **The role of XRCC1 in the repair of DNA strand breaks in skeletal muscle differentiation.**

Leanne E. Burns

This thesis is submitted to the Faculty of Graduate and Postdoctoral Studies  
in partial fulfillment of the requirements for a Master of Science degree in  
Cellular and Molecular Medicine.

Department of Cellular and Molecular Medicine  
Faculty of Medicine  
University of Ottawa  
June 30, 2011

© Leanne E. Burns, Ottawa, Canada, 2011

## **Abstract**

Caspase-3 has demonstrated a non-apoptotic function in several developmental programs including skeletal muscle differentiation, yet the mechanism of action has not been fully elucidated. Under apoptotic conditions Caspase-3 induces DNA fragmentation through activation of CAD. Recent observations have demonstrated CAD activity and the resulting DNA strand breaks are also vital for skeletal muscle differentiation. These breaks are transient in nature, suggesting an active DNA repair program to maintain genomic integrity. The aim of this study was to delineate the DNA repair mechanism coordinated with caspase/CAD mediated DNA damage. It was found that XRCC1 formed punctate nuclear foci early in myoblast differentiation concurrent to the induction of DNA damage. Caspase-3 inhibition caused attenuation of the formation of DNA lesions and XRCC1 foci in differentiating myoblasts. Targeted reduction in XRCC1 expression impaired myoblast differentiation. These results suggest that XRCC1 may play a role in repairing the DNA damage associated with myoblast differentiation.

# Table of Contents

1	Introduction .....	1
1.1	Myogenesis .....	2
1.1.1	Genetic regulation of myogenesis .....	5
1.2	Caspase activity as a cell fate determinant.....	7
1.2.1	Nuclear events in apoptosis.....	10
1.2.2	Non-apoptotic roles for caspases .....	11
1.3	DNA damage and DNA repair in gene regulation .....	15
1.3.1	V(D)J recombination .....	18
1.3.2	Chromosome switching in meiosis .....	18
1.3.3	Gene activation by components of DNA damage and repair.....	20
1.4	DNA repair mechanisms in eukaryotes.....	22
1.4.1	Repair of DNA double strand breaks .....	25
1.4.2	The repair of single strand DNA lesions.....	26
1.5	Hypothesis and Aims .....	28
1.5.1	Hypothesis.....	28
1.5.2	Aims.....	28
2	Materials and Methods.....	29
2.1	Tissue culture .....	30
2.1.1	C2C12 plating and passaging .....	30
2.1.2	Primary Myoblast Isolation.....	31
2.2	Nucleic acid isolation and expression analysis.....	32
2.2.1	RNA isolation from cultured cells .....	32
2.2.2	First strand cDNA synthesis .....	33
2.2.3	Reverse Transcription Polymerase Chain Reaction (RT PCR) .....	34
2.2.4	Quantitative Real time RT PCR.....	35
2.3	Protein isolation and expression analysis .....	36
2.3.1	Protein lysate collection and measurement of concentration.....	36
2.3.2	Western Blot Analysis of Protein Expression.....	37
2.4	Single cell gel electrophoresis .....	38

2.5	In situ nick translation .....	40
2.6	shRNA mediated knock down of XRCC1 .....	41
2.7	Inhibition of caspase 3 .....	42
2.8	Immunofluorescent staining .....	42
3	Results.....	44
3.1	Temporal location of DNA damage in skeletal muscle differentiation.....	45
3.2	Expression of DNA repair proteins during differentiation of skeletal myoblasts 49	
3.3	The effect of caspase 3 inhibition on XRCC1 foci formation during myoblast differentiation .....	58
3.4	The effect of shRNA mediated knock down of XRCC1 gene expression in differentiating myoblasts.....	63
4	Discussion.....	67
4.1	The role of Caspase 3 and Caspase Activated Nuclease in the formation of DNA lesions during cellular differentiation.....	68
4.2	Gene activation and the role of DNA repair proteins .....	70
4.2.1	Single strand break repair proteins .....	70
4.2.2	Double strand break repair proteins .....	72
4.3	XRCC1 and its possible contribution to DNA damage repair in skeletal muscle differentiation. ....	74
4.4	Future experimental directions to elucidate candidate repair pathways/proteins that moderate cell differentiation .....	77
4.5	Final Summary and Conclusion .....	79
5	References .....	81
6	Appendix.....	86

## Table of Figures

Figure 1 Adult skeletal muscle differentiation.....	4
Figure 2 Intrinsic and extrinsic activation of the caspase cascade results in the activation of effector caspase 3 and the induction of apoptosis. ....	9
Figure 3 DNA damage and repair occurs in normal biological processes in mechanisms that are beneficial to the cell.....	17
Figure 4 Eukaryotic DNA repair mechanisms .....	24
Figure 5 Single cell gel electrophoresis in primary myoblast and C2C12 myoblast cells over the differentiation time course reveals the temporal location of transient DNA lesions. ....	48
Figure 6 RT PCR gene expression analysis of DNA repair protein candidates in differentiating C2C12 cells.....	53
Figure 7 DNA ligase IV and 53BP1 immunofluorescent staining in C2C12 myoblast cells does not reveal a change in protein localization following induction of differentiation. 54	
Figure 8 XRCC1 forms distinct nuclear foci early in skeletal muscle differentiation in C2C12 cells upon low serum induction of differentiation.....	55
Figure 9 Protein and gene expression of XRCC1 and DNA ligase IV in differentiating C2C12 myoblast cells. ....	56
Figure 10 Co staining for XRCC1 foci formation and <i>in situ</i> nick translation assay in C2C12 myoblast cells over differentiation reveals that XRCC1 foci form following DNA damage. ....	57
Figure 11 Immunofluorescent staining for XRCC1 in caspase 3 inhibited differentiating C2C12 cells reveals a reduction in foci formation when caspase 3 is inhibited. ....	60
Figure 12 DNA damage and XRCC1 foci formation is blocked by chemical inhibition of caspase 3 in differentiating C2C12 cells. ....	61
Figure 13 DNA damage is reduced when caspase 3 is chemically inhibited in differentiating C2C12 myoblast cells as seen by a reduction in comet tail length. ....	62
Figure 14 shRNA mediated knock down of XRCC1 in differentiating C2C12 myoblast cells impairs the formation of myotubes.....	65

Figure 15 Graphical analysis of shRNA mediated knock down of XRCC1 in differentiating C2C12 myoblasts..... 66

## List of abbreviations

ANOVA	analysis of variance
AOA1	ataxia with oculomotor apaxia
Apaf-1	apoptotic protease activating factor 1
ATM	ataxia telangiectasia mutated
ATR	ataxia telangiectasia and Rad3-related protein
B-NHEJ	backup-non-homologous end joining
Bid	Interacting domain death agonist
BRCA1	breast cancer suppressor protein 1
BRCT	BRCA c-terminus
BSA	bovine serum albumin
CAD	caspase activated nuclease
CDK	cyclin dependent kinase
ChIP	chromatin immunoprecipitation
D loop	displacement loop
DAPI	4',6-Diamidino-2-phenylindole dihydrochloride
DISC	death-inducing signaling complex
DM	differentiation media
DMSO	dimethyl sulphoxide
DDR	DNA damage response
DNA PK	DNA protein kinase
DNA PKcs	DNA protien kinase catalytic subunit
D-NHEJ	DNA PK dependant non-homologous end joining
DR5	Death receptor 5
DSBR	double strand break repair
ER2	estrogen receptor 2
ERE	estrogen response element
FADD	FAS associated death domain
GM	growth media
HGF	Hepatocyte growth factor
HJ	Holliday junction
HMG	high mobility group protein
HMGB	high mobility group B protein
HRR	homologous recombination-mediated repair
HS	horse serum
ICAD	inhibitor of caspase activated nuclease
IP	immunoprecipitation
ISNT	<i>in situ</i> nick translation

KD	knock down
KO	knock out
MAPK	myogen-activated protein kinase
MEF2	myocyte enhancer factor 2
MRF	myogenic regulatory factor
MyHC	myosin heavy chain
NHEJ	non-homologous end joining
PARP	poly (ADP-ribose) polymerase
PNK	poly nucleotide kinase
qPCR	quantitative polymerase chain reaction
RAG(1-2)	recombination-activating-gene protein 1-2
RSS	recombinational signal sequence
RT PCR	reverse transcription polymerase chain reaction
SCAN1	spinocerebellar ataxia with axonal neuropathy
shRNA	small hairpin ribonucleic acid
SSBR	single strand break repair
TCF	T cell transcription factor
TpopII $\beta$	topoisomerase II $\beta$
TRAIL	Tumour necrosis factor related apoptosis-inducing ligand
V(D)J	variable(diversity)joining
XRCC1	x-ray repair cross complimenting protein 1

## **Acknowledgements**

I would like to start by thanking my supervisor Dr Lynn Megeney for first taking me in as an undergrad summer student. My experience in the lab in those early years is what sparked my interest in graduate studies and opened my eyes to the inspiring world of scientific research. Thank you to my thesis advisory committee, Dr Jeff Dilworth and Dr David Picketts. Thank you to Brian for all the guidance and advice you have offered me over the years. Without your support I would likely have crumbled under the pressure. Thank you, thank you, thank you. Thanks to all my lab mates past and present especially Becca, Sarah, Steve and Jen. You have made this experience a lot of fun. I can't wait to see what great things life has in store for you all. Thank you to my friends and family who have helped me to find balance in my life outside of the lab. To my Mom and Dad, whose enthusiasm and confidence in me have pushed me to go further than I ever imagined I was capable of, I will always be grateful. Finally to Matthew, thank you for your unwavering support over the years. Without you none of this would have been possible, I owe you big time!

# **1 Introduction**

Cellular differentiation is the process which gives rise to all the specialized cell types found in a complex organism. In general, the differentiation process is mediated by a controlled progression of gene expression, dependent on both lineage specific events as well as alterations that are conserved across varied cell types. Concurrent with the process of differentiation is the process of cell death or apoptosis, which further serves in shaping the organism through the removal of unwanted cells. Interestingly, apoptosis and the differentiation process also share a high degree of morphological similarity, suggesting that these disparate cell fates may utilize a common genetic program.

Skeletal muscle differentiation, or myogenesis, serves as an ideal model system to explore the tenets of cellular differentiation. Utilizing this model, Fernando et al. made one of the early observations that the catalytic activity of the cysteine protease, caspase 3, participated in non death cellular events (Fernando, Kelly et al. 2002). Further, this activity was linked to the activation of the caspase-activated nuclease (CAD), an enzyme that generates wide spread DNA fragmentation to the myoblast genome, an event that is required for the differentiation process to proceed (Larsen, Rampalli et al. 2010). The transient nature of these strand breaks indicates an active DNA repair process at work, the mechanism of which will be explored in this thesis.

## ***1.1 Myogenesis***

During vertebrate development skeletal muscle originates from somites distributed alongside the neural tube that eventually become the myotome. Cells located in the dorsal myotome, termed the dermomyotome, will give rise to the skeletal

muscle of the trunk and limbs. These cells migrate into the limb buds, proliferate, activate the expression of myogenic determination factors, and ultimately differentiate into functional skeletal muscle (Buckingham, Bajard et al. 2003).

Skeletal muscle differentiation can occur in adult muscle in response to injury or stress. A satellite cell (SC) population exists under the basal lamina of adult muscle fibers; these cells will activate in response to the injury stimuli. Once activated these skeletal muscle precursor cells, called myoblasts, undergo several rounds of replication and move into the site of damage. Once located to the site of damage these cells will differentiate and fuse with existing cells to repair the injury (Hill, Wernig et al. 2003).

Committed myoblast progenitor cells will proliferate in the presence of growth factors including fibroblast growth factors. Once these growth factors have been depleted the myoblasts will exit the cell cycle and will no longer divide. The cells begin to align with neighbouring myoblasts and will fuse to form myotubes. The resulting multinucleated myotubes will further organize into muscle fibers that eventually will begin to spontaneously contract (Gilbert, 2000). A characteristic profile of transcription factors mark and regulate the progression of this event as outlined in Figure 1.

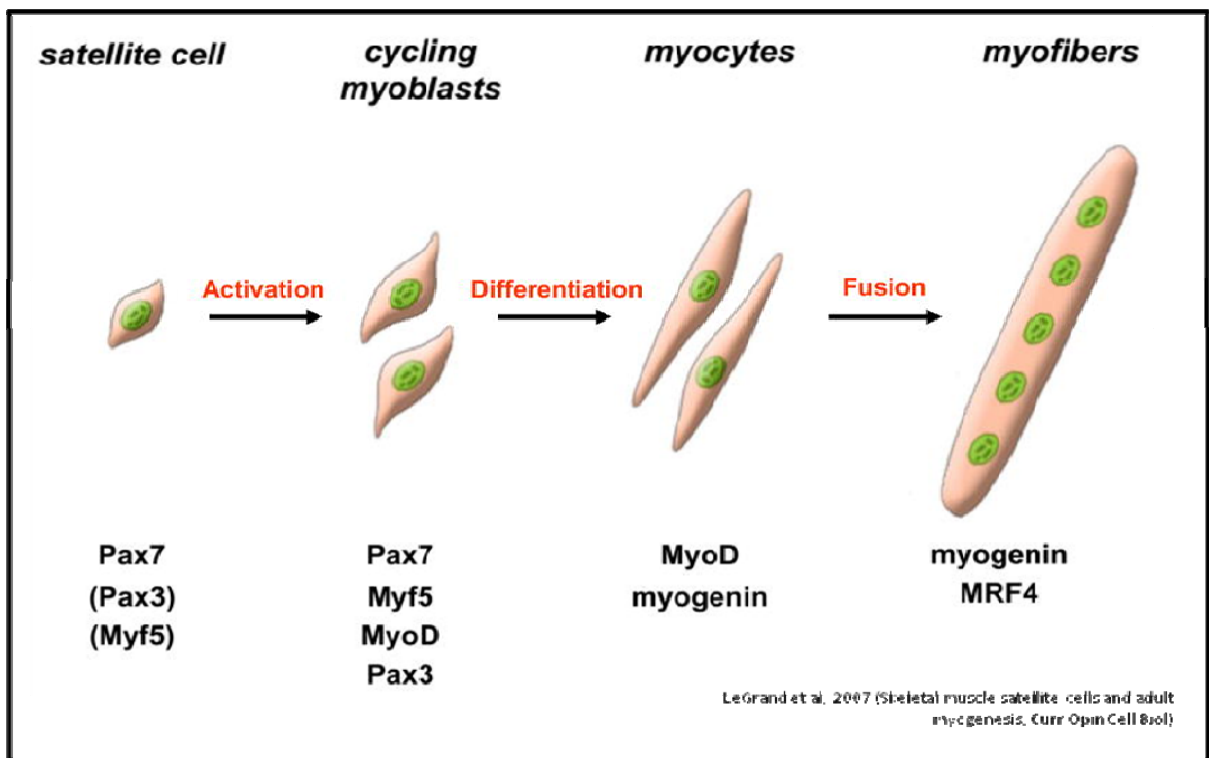


**Figure 1 Adult skeletal muscle differentiation.**

The progression of adult muscle satellite cells through differentiation to committed myofibers requires tight regulation of myogenic regulation factors and Pax genes. Copyright license number: 2693201285578

### **1.1.1 Genetic regulation of myogenesis**

In adult muscle tissue the SC population resides in the basal lamina where they have limited gene expression and protein synthesis. Upon stress, due to muscle injury or disease, the cells become active via a mechanism that is not well known (Hill, Wernig et al. 2003). Growth factors such as fibroblast growth factor (FGF) are required for SC activation as they are able to induce the p38 $\alpha$ / $\beta$  MAPK signal cascade which is a known requirement for SC activation (Penn, Bergstrom et al. 2004). Hepatocyte growth factor (HGF), activated by mechanical fiber stretch and the resulting increase in nitric oxide synthesis, causes the downregulation of myostatin which is a negative regulator of myogenesis (Tatsumi, Hattori et al. 2002). With myostatin downregulated the SC are able to exit their quiescent state. The newly activated SC will exit the basal lamina and will upregulate the expression of both Pax7 and MyoD (Seale, Sabourin et al. 2000). With this gene expression profile the cells will proliferate through several rounds of cell division. During this time the cells begin to downregulate Pax7 and upregulate myogenin expression. Once this occurs the SC will exit the cell cycle and will begin myogenesis (Le Grand and Rudnicki 2007). A small population of the cells will retain Pax7 expression and lose the expression of myogenic markers. These cells will exit the cell cycle to a quiescent state and serve as a reservoir to repopulate the SC niche (Olguin and Olwin 2004).

Myogenesis is coordinated by the activation of the muscle specific myogenic regulatory factors (MRFs) which include MyoD, Myf5, Mrf4 and myogenin and the downregulation of Pax3/7 (Bergstrom and Tapscott 2001). In muscle satellite cell

populations the transcription factors Pax7 and Myf5 are expressed. The expression of Myf5 is controlled by Pax3 and acts to direct the precursor cells to a muscle lineage in the developing embryo. Pax7 is important for the maintenance of the satellite cell population as it directs SC self renewal (Kuang, Charge et al. 2006). The myogenic regulatory factors become active through various cues in the progression of myogenesis. The cells that will go on to become mature muscle cells express Myf5 and will downregulate Pax7 releasing the cell survival signals and allowing for the upregulation of MyoD and, shortly thereafter, myogenin (Cornelison and Wold 1997). The upregulation of myogenin acts to further downregulate Pax7 expression in myocytes (Otto, Collins-Hooper et al. 2009). MyoD is required for the differentiation of cycling myoblasts (Sabourin, Girgis-Gabardo et al. 1999) whereas Myf5 regulates proliferation and exit of the cell cycle (Gayraud-Morel, Chretien et al. 2007). The remaining two MRFs, myogenin and MRF4, are required for the transformation of the myoblast into fused, multi nucleated myotubes and are expressed only when the cells have transformed into myocytes (Le Grand and Rudnicki 2007).

The activation of the MRFs results in the downstream activation of structural genes and regulatory elements ultimately leading to the formation of functional muscle tissue. In embryonic development the myogenic precursor cells are led to a committed lineage via signals generated in surrounding tissues. Such signals include Wnt and sonic hedgehog signal cascades which act to upregulate MyoD family transcription factors (Munsterberg, Kitajewski et al. 1995). It has been shown that p38 myogen-activated protein kinase (MAPK) signaling is involved in cells expressing MyoD (Wu, Woodring et

al. 2000). Originally it was thought that the p38 pathway was involved in stress response and the initiation of apoptosis exclusively but it has been shown that both p38 $\alpha$  and p38 $\beta$  play an important role in myogenesis and are likely to contribute to the exit of the cell cycle that occurs in differentiating myoblasts (Keren, Tamir et al. 2006).

## ***1.2 Caspase activity as a cell fate determinant***

Caspases are a family of cysteine proteases, which reside within the cell in a catalytically inactive form until proteolytically processed into an active form. This activation has been well characterized in the induction of apoptosis originating from intrinsic or extrinsic signaling (Taylor, Cullen et al. 2008). Newly emerging data suggests that caspases also play an important role in cellular differentiation but the exact mechanism through which the caspases act is not fully understood. Caspase 3 in particular has been implicated in the differentiation of many mammalian cell types including skeletal muscle (Fernando, Kelly et al. 2002). Caspase 3 is the effector caspase that is activated through the induction of either the intrinsic or extrinsic pathway (Figure 2). Intrinsic caspase activation is stimulated by the release of cytochrome c from the mitochondria which facilitates the formation of the apoptosome. Bcl-2 is a protein which acts to inhibit the release of cytochrome c from the mitochondria by maintaining the integrity of the outer membrane. This protein can be inhibited by BH3 family proteins when expressed above a crucial threshold within the cytoplasm (Chao and Korsmeyer 1998). The apoptosome complex consists of apoptotic protease activating factor 1 (Apaf-1) and ATP which bind with procaspase 9 resulting in initiator caspase

activation. In turn, the activated apoptosome engages the effector caspase 3 (Adrain and Martin 2001).

The extrinsic pathway is exemplified by signaling through the Fas receptor, in which binding of the Fas ligand induces the assembly of the death-inducing signaling complex (DISC). The DISC consists of the Fas associated protein with death domain (FADD) and caspase 8. Caspase 8 is activated via an autoactivation process whereby individual caspase 8 proteins cross cleave and dimerize to form the fully activated protease. The activated caspase 8 dimer is then able to activate the caspase 3 zymogen (Chinnaiyan, O'Rourke et al. 1995). Once activated caspase 3 will act on many downstream protein targets by cleavage activating or inactivating steps. Activated caspase 8 also bridges crosstalk between the intrinsic and extrinsic pathways by activating Bid (interacting domain death agonist). Activated Bid is able to facilitate the release of cytochrome c from the mitochondria (Yi, Yin et al. 2003).

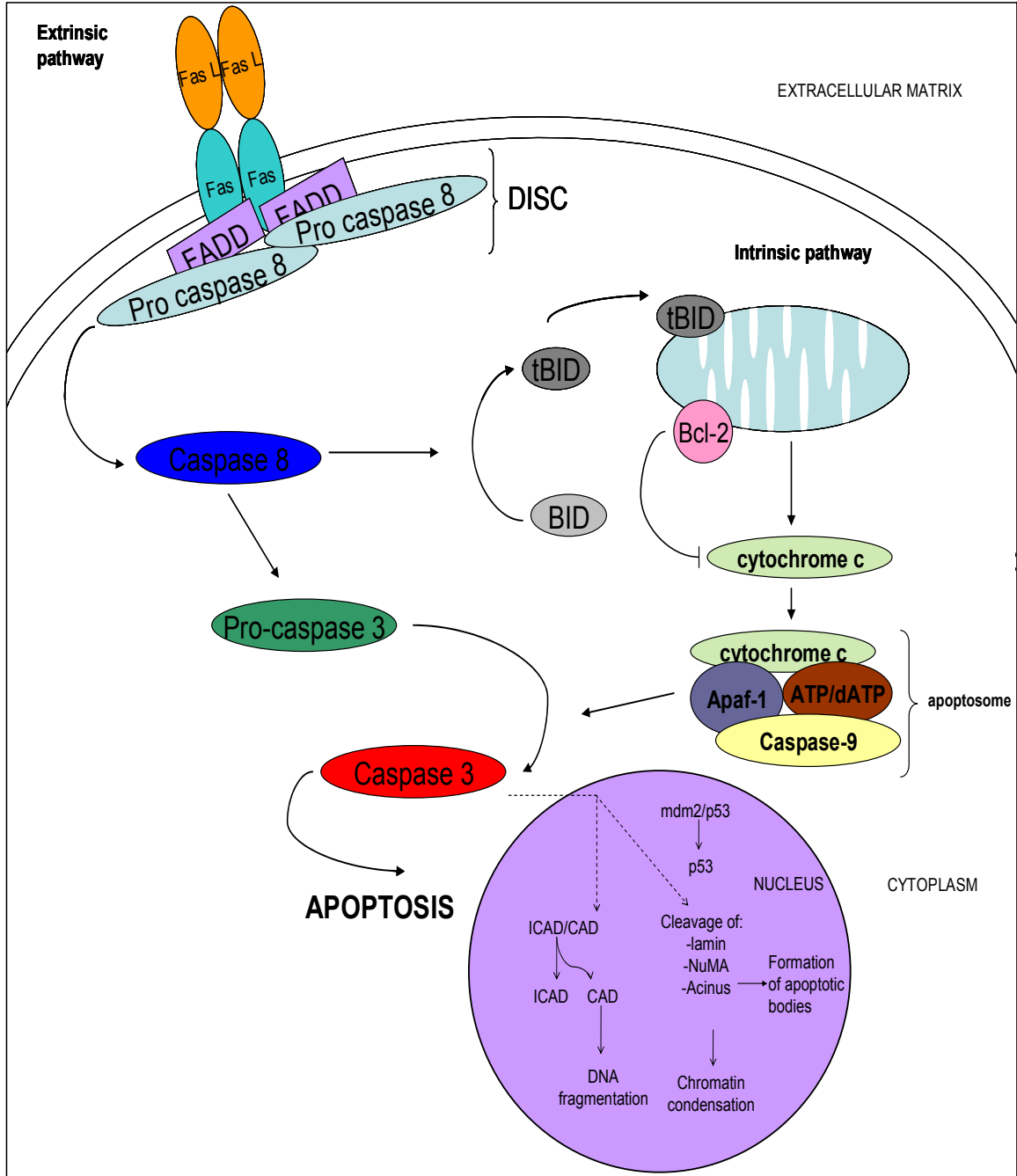


Figure 2 Intrinsic and extrinsic activation of the caspase cascade results in the activation of effector caspase 3 and the induction of apoptosis.

### ***1.3 Nuclear events in apoptosis***

As an effector caspase, caspase 3 directs numerous downstream molecular events in apoptosis that manifest in the cytoplasmic and nuclear breakdown of the cell. Specifically, apoptotic caspase 3 activation culminates in the signaling of chromatin condensation and DNA fragmentation as outlined in Figure 2 (Robertson, Orrenius et al. 2000). Although a number of nucleases have been reported to inflict DNA fragmentation under apoptotic conditions, caspase 3 activity primarily activates the caspase activated DNase (CAD) in this setting. CAD and its nascent inhibitor ICAD (inhibitor of caspase activated DNase) form a complex, whereby the nuclease remains inactive. This inhibition is released when ICAD is targeted for cleavage by caspase 3, releasing CAD to form an active homo dimer with an active scissor-like conformation that begins the fragmentation of the genome (Enari, Sakahira et al. 1998). During apoptosis, caspase 3 can inactivate, through cleavage, a number of proteins that participate in DNA repair, including PARP (poly(ADP ribosyl)ation protein) and DNA-PK. This allows DNA damage to accumulate without counterproductive DNA repair (Oliver, de la Rubia et al. 1998). This inactivation may also serve as a safe guard against the survival of the cell that may have accumulated dangerous genetic lesions following CAD activation.

Nuclear disintegration concurrent with DNA fragmentation is also directed by caspase activity. Here, cleavage of protein substrates that maintain the structural integrity contribute to nuclear collapse. The cleavage of these structural proteins including lamins, NuMa, Acinus and SATB1 also participate in DNA fragmentation as

these proteins have been demonstrated to constrain or protect the genome from CAD access (Robertson, Orrenius et al. 2000). The cleavage of DNA by apoptotic nucleases such as CAD is not dependent on primary DNA sequence but rather upon the local genomic topology. As such if the DNA remains tightly integrated into chromatin structures then nucleases will be restricted in the ability to access DNA and induce strand breaks. Additional proteins are responsible for the condensation of the chromatin which facilitate CAD by opening up the chromatin to allow strand breaks (Sakahira, Enari et al. 1999). Indeed, CAD alone has limited ability to affect DNA laddering during apoptosis.

In response to cellular stress the tumour suppressor p53 transcription factor is activated resulting in an exit of the cell from the cell cycle and, when the cell is under extreme stress, will aid to trigger the apoptotic cascade via both extrinsic and intrinsic pathways. As well as being able to trigger an apoptotic response in stressed cells p53 has also been implicated in cellular differentiation and in the DNA damage response. Under normal conditions p53 is kept inactive by its suppressor mdm2 which inhibits the transcriptional activity of p53 (Haupt, Berger et al. 2003).

### **1.3.1 Non-apoptotic roles for caspases**

In addition to the established role in apoptosis, caspase activities have been implicated in a number of cellular processes, particularly cellular differentiation. For example, enucleation during the differentiation of a number of cell types, including lens cells, erythrocytes and platelet cells, requires caspase activity (Ishizaki, Jacobson et al. 1998; Zermati, Garrido et al. 2001) (Li and Yuan 2008). This form of differentiation is

considered as a partial form of apoptosis, yet the differentiation of cell lineages that lack a more overt apoptotic phenotype are also reliant on caspase activation. Although less apparent than cellular differentiation that involves enucleation many similarities between these differentiation events and apoptosis can be observed such as remodeling of the microtubules, membrane deformations and morphological changes that occur in the nucleus (Fernando and Megeney 2007). Caspase 3 in particular has been implicated in the differentiation of osteoblasts, neurons, cardiac muscle and skeletal muscle as well as in embryonic and hematopoietic stem cells (Szymczyk, Freeman et al. 2006; Fujita, Crane et al. 2008; Li and Yuan 2008; Abdul-Ghani, Dufort et al. 2011).

Caspase directed cell differentiation may arise from either a direct stimulation of differentiation specific signals and/or by limiting progenitor cell/stem cell self renewal but the mechanism by which caspases are able to induce differentiation is not yet understood and requires further investigation (Li and Yuan 2008). The role of caspase 3 in the differentiation of skeletal muscle and neurons has been proven to be critical for successful differentiation. When caspase 3 is inhibited there is a significant reduction in differentiation observed in both neurosphere and skeletal muscle cultures (Fernando, Brunette et al. 2005). Both caspase 3 and caspase 8 display transient activation patterns during early stages of the myoblast differentiation program. In caspase 3 gene targeted mice as well as in caspase 3 chemically inhibited myoblast cultures there is a marked inability of the cells to undergo normal differentiation. Blockade of caspase 8 did not limit myoblast differentiation to the same extent as targeted inactivation of caspase 3. Early studies indicate that caspase 3 may be involved in activating the p38 MAPK

pathway that causes cells to exit the cell cycle, a step that is required for differentiation to progress (Fernando, Kelly et al. 2002). The proposed mechanism of MAPK activation is through MST1 cleavage activation by caspase 3 early in the differentiation time course. Mammalian sterile twenty-like kinase 1 (MST1) is able to act upstream of MAPK activation by targeting MKK6 and members of the p38 MAPK family (Graves, Gotoh et al. 1998). It has been shown that MST1 is activated in differentiating C2C12 cells and when caspase 3 is inhibited the MST1 activation is no longer detected. MST1 was also demonstrated to have a rescue effect in the transfection of active MST1 kinase into caspase 3 null myoblast cells. These cells were observed to have gained the ability to undergo differentiation upon successful transfection (Fernando, Kelly et al. 2002). These preliminary studies indicated a cell autonomous role for caspase 3 activation and, a non-death role for caspase 3 in the differentiation protocol.

The intrinsic apoptotic pathway initiator caspase 9 has also been implicated in the activation of caspase 3 in muscle differentiation. It was discovered that when caspase 9 expression was knocked down in C2C12 cells there was an observed delay in the fusion events that occur late in the differentiation process. Similarly, when Bcl-xL (known to inhibit caspase 9 by inhibiting the release of cytochrome c from the mitochondrion (Finucane, Bossy-Wetzel et al. 1999)) was up-regulated a similar delay in fusion was observed. As only a delay and not a total blockade of fusion was observed by removing caspase 9 activity in differentiating myoblasts, these observations suggest that more than one caspase 3 activation pathway may be working in concert to promote skeletal muscle differentiation (Murray, McMahon et al. 2008).

Similarly, the extrinsic apoptosis pathway has been implicated in the myoblast differentiation process. Here, a study out of the Weymann lab in 2009 noted that the TRAIL receptor DR5/FADD/caspase pathway was able to regulate the expression of MyoD. In the classical apoptosis cascade the extrinsic pathway culminates in the activation of caspase 3 via caspase 8. Caspase 8 is activated through signaling in the death ligand TRAIL (tumour necrosis factor related apoptosis-inducing ligand) and death receptor 5 (DR5). DR5 signals to FADD which is responsible for caspase 8 activation. It has been demonstrated in both FADD and DR5 dominant negative mutants that not only is the ability of the mutants to differentiate abrogated but the expression of MyoD is reduced compared to control cells that were induced to differentiate using exposure to low serum media conditions (Freer-Prokop, O'Flaherty et al. 2009).

Although the role of caspase 3 in skeletal myoblast differentiation has been well documented, other cell types appear to be equally dependent on caspase mediated differentiation. Neuronal differentiation activates caspase 3 in part to signal the activity the protein kinase p38 $\alpha$ . This is an important observation as p38 is responsible for the downstream phosphorylation and activation of many targets required for neuronal differentiation such as myocyte enhancer factor 2 (MEF2) family of proteins (Fernando, Brunette et al. 2005). More recently, cardiomyocytes have been reported to utilize non-canonical Wnt signaling to engage caspase activity, which then targets and cleaves beta-catenin to abrogate canonical Wnt activity. This in turn leads to the specialized development of cardiomyocytes into the myocardium (Abdul-Ghani, Dufort et al. 2011).

Additional studies have examined the mechanism by which caspase 3 may engage the differentiation program. Larsen *et al* found that caspase activated DNase (CAD) is in fact activated upon induction of skeletal myoblast differentiation and that CAD activation is absolutely required for the differentiation program to proceed. As noted previously, CAD activity in apoptotic cells is the primary biochemical mechanism to induce DNA lesions. These lesions, in part, result in the hallmark 200bp laddering effect that is observed when the DNA lysates are subject to gel electrophoresis. Larsen *et al* have shown that DNA lesions are present throughout early stages of myoblast differentiation. Moreover, reduced expression of CAD leads to a substantial reduction in the formation of these DNA lesions concurrent to impaired myoblast differentiation. Investigation of possible gene targets of CAD revealed that the p21 promoter region was subject to a CAD induced DNA strand break (Larsen, Rampalli et al. 2010). The p21 promoter region represents an important target, as enhanced p21 expression induces cell cycle exit during the initiation of differentiation (Zhang, Wong et al. 1999). The study by Larsen *et al* clearly establishes that regulated DNA damage is a prerequisite for myoblast differentiation. Nevertheless, it remains unclear by which mechanism a myoblast repairs these transient DNA lesions. Indeed, this is a critical issue as differentiated myofibers are long lived cells types, a feature that will require maintenance of genome integrity.

#### ***1.4 DNA damage and DNA repair in gene regulation***

Interestingly, DNA damage in general has been reported to induce stem cells to terminally differentiate. For example, extensive DNA damage in melanocyte stem cells

prompts cell cycle exit and differentiation to mature melanocytes rather than undergoing apoptosis as might be expected (Inomata, Aoto et al. 2009). Similarly, in *Drosophila* cell cultures treated with DNA damage inducing chemicals cell differentiation was enhanced suggesting that the DNA strand breaks may have triggered the change in cell fate (Hossain, Akimitsu et al. 2003). What remains unclear is how the induction of DNA damage can induce cellular differentiation. One possibility is that the strand break itself may lead to the activation or inactivation of a specific gene. Alternatively, DNA damage may elicit a more global alteration whereby the strand breaks enhance or impair genome accessibility across multiple loci. The idea that DNA damage is involved in normal biological processes is not a novel concept. Specifically there are many accounts of DNA damage being applied for the benefit of an organism such as in V(D)J recombination in immune cells to generate the diversity of antibody responses and in the crossing over events that occur between homologous chromosomes in meiosis as outlined in Figure 3.

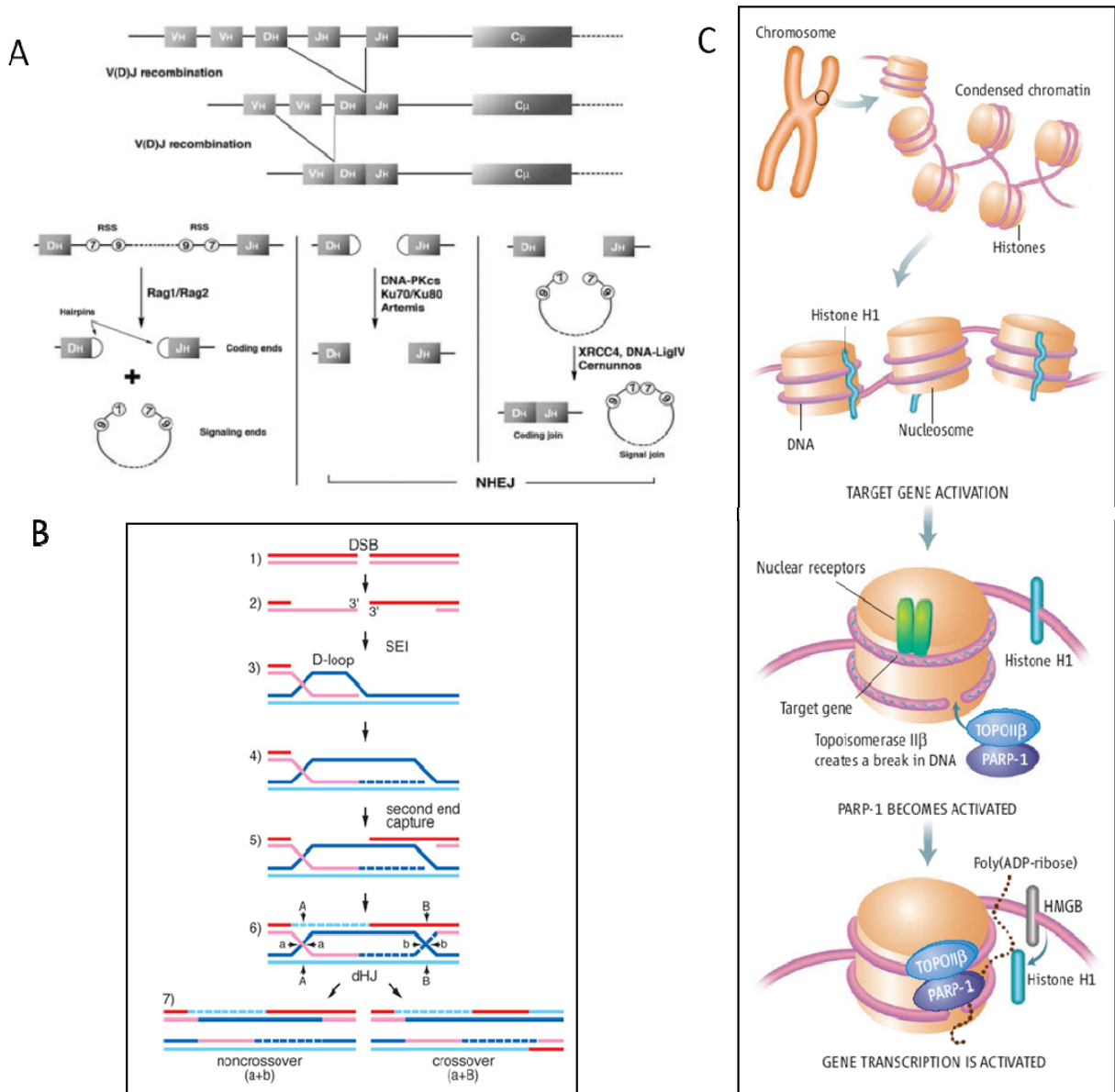


**Figure 3 DNA damage and repair occurs in normal biological processes in mechanisms that are beneficial to the cell.**

A) In the B and T cells of the immune system V(D)J recombination confers the vast antigenic diversity that is a hallmark of the adaptive immune system (Rivera-Munoz, Malivert et al. 2007). Reprinted with permission from John Wiley and Sons 2747130520793 . B) In meiosis crossing over occurs to ensure that the genetic material within the gametes is varied and contains DNA from both maternal and paternal chromosomes. This ensures that when offspring are created that there is variance among individuals (Whitby 2005). Reprinted with permission from Portland Press. C) Genes are typically located amid a tightly packed chromatin structure and in order to be transcribed they need to become more accessible. In some cases genes are activated after DNA lesions are created in the nucleosome by TOP2II $\beta$  so that a HMGB protein can replace histone H1 and open up the nucleosome allowing particular genes to be accessed by transcription machinery. From (Haince, Rouleau et al. 2006). Reprinted with permission from AAAS.

### **1.4.1 V(D)J recombination**

V(D)J recombination is one such example where the induction of double stranded DNA breaks allows gene segments to be rearranged to gain antigenic diversity (Figure 3 A). This process begins in the lymphoid cells when recombination-activating – gene proteins 1 and 2 (RAG1, RAG2) cleave DNA at conserved recombination signal sequences (RSS). These sequences are found to flank all antigen-receptor variable-region gene segments and, when cleaved, coding and RSS ends are generated. The RSS ends go on to be precisely ligated while the coding ends are processed in such a way that may involve nucleotide loss or gain as well as ligation. It is this addition or removal of nucleotides that confers the genetic variations within the variable (V), diversity (D) and joining (J) gene segments (Gellert 2002). The gene ligations employ the DNA repair mechanism of non-homologous end joining where the D and J segments are first joined followed by the joining of the newly formed DJ segment with the V segment. In the first steps of the repair process the Artemis protein forms a complex with DNA PKcs which subsequently activates Artemis. The activation of Artemis is required to exploit its endogenous endonuclease activity, a step that initiates the formation of antigen receptor diversity that is the hallmark of V(D)J recombination. Additional core elements of NHEJ are then recruited and the ligations are sealed by DNA ligase IV and XRCC4 (Weterings and Chen 2008).

### **1.4.2 Chromosome switching in meiosis**

During meiosis genetic material from a paternal chromosome is exchanged with material from maternal chromosome via homologous recombination that occurs in

meiosis I. This exchange of genetic material is what adds variation in the offspring of eukaryotes. Figure 3B shows how the formation of double stranded breaks in the chromosome are repaired using the homologous DNA strand as the template to which the DNA will be repaired.

The crossing over mechanism has multiple functions within the cell; these include promotion of genetic diversity, removal of deleterious mutations and the formation of chiasmata which are important in the formation of attachments of chromosomes to the polar spindle in the first round of segregation in meiosis. Defects in attachment can lead to aneuploidy in gametes (Carvalho 2003). Once a double strand break is formed in one of the homologues the broken ends are degraded from the 5' end to result in single stranded tails with 3' OH ends. The tail locates to the homologous sequence on the homologous chromosome and invades it to form a displacement loop (D loop). DNA synthesis fills in the remaining gaps by extending the D loop so that it can anneal to the single stranded tail that is left open on the other side of the break. Synthesis and ligation of the dsDNA breaks results in the connection of homologues by Holliday junctions (HJ). The HJ are separated by cleavage of symmetrical strands at each junction leaving maternal DNA on one side of the HJ and paternal DNA on the other. This constitutes a new combination of genetic material in the resulting alleles and allows for the formation of a chiasmata which will help guide the homologues to the meiosis I spindle. The formation of a chiasmata will only occur if the HJ are cleaved at symmetrical strands and not on the same pair of strands. If this occurs crossing over has not occurred and no chiasmata is formed (Whitby 2005).

### **1.4.3 Gene activation by components of DNA damage and repair**

DNA damage has also been shown to be a pre-requisite for altering the transcription of certain genes. For example, in order for the cell to accommodate the vast amount of DNA that comprises our genome it has evolved a method to store the DNA in such a way that it is compacted into strands of DNA wound around histone cores and further wound into coils and, subsequently, into chromosomes. This presents a problem to the cell when it requires access to a particular region of the genome for gene transcription. It has been proposed that the formation of DNA strand breaks may facilitate the opening of the genome so that transcription factors and related transcription machinery can access genes that are wound into the nucleosome (Figure 3C) (Haince, Rouleau et al. 2006).

One mechanism, described by Ju *et al*, utilizes Topoisomerase II Beta along with PARP and DNA PK to induce a strand break in the DNA that winds around the nucleosome in order to provide access to the genes contained within. The DNA lesion itself is induced by TopoII $\beta$  while PARP and DNA PK recognize the lesion and cause a relaxation in the chromatin to facilitate transcription (Ju, Lunyak et al. 2006).

Here, the role of PARP goes beyond simple recognition of the strand break, in that PARP is responsible for the poly(ADP ribosyl)ation of itself and histones H1, H2A and H2B. This induces a relaxation of the chromatin structure surrounding the addition of the poly(ADP robose). The relaxation of the chromatin allows for access of repair proteins to the sites of DNA damage in a typical DNA damage response. Similarly PARP is hypothesized to stimulate gene activation by promoting the exchange of histone H1

for high mobility group B protein (HMGB). HMGB is a chromatin associated nucleoprotein that binds to the DNA to facilitate the binding of transcription factors to their DNA targets while H1 is a known repressor of transcription therefore the replacement promotes the transcription of the exposed chromatin (Ju, Lunyak et al. 2006).

Specifically topoisomerase II $\beta$  has been demonstrated to cause transient DNA lesions in the promoter region of the 17 $\beta$ -estradiol (E<sub>2</sub>) induced gene pS2 in Michigan Cancer Foundation (MCF)-7 cells. Following E<sub>2</sub> stimulation of MCF-7 cells, the pS2 promoter region is subject to strand breaks. The damage followed by PARP recruitment and H1-HMGB replacement leads to the upregulation of pS2 expression by relieving chromatin compaction so that the E<sub>2</sub> activated transcription factor ER $\alpha$  is able to bind the estrogen response element (ERE) found within the promoter region. The authors also demonstrated that the same mechanism is responsible for the upregulation of androgen receptor, retinoic acid receptor, thyroid receptor and activating protein 1 dependant transcriptional activation where they found that the TopoII $\beta$ /PARP machinery was found to localize to the promoter regions of these genes upon induction of expression (Ju, Lunyak et al. 2006). Another study that looked at gene expression in TopoII $\beta$  knock out mice found that there was little change in gene expression overall. Upon closer examination of the effected genes they found that almost all of the genes with altered expression were developmentally regulated and implicated in numerous differentiation pathways. There was little effect found on the expression of housekeeping genes when TopoII $\beta$  activity was ablated (Lyu, Lin et al. 2006). Finally,

single strand breaks in the promoter region of the VEGF gene have been shown to increase the torsional flexibility of the gene which allows for the incorporation and binding of chromatin remodeling factors which cause a further opening up the chromatin so that it can be accessed for transcription (Ziel, Grishko et al. 2005).

### ***1.5 DNA repair mechanisms in eukaryotes***

Eukaryotic cells are subject to multiple genotoxic events, including errors in DNA replication, site specific recombination, reactive oxygen species, exogenous ionizing radiation or a variety of mutagenic chemicals. As such there are a number of mechanisms deployed to repair damaged DNA throughout the life cycle of a cell (Iliakis, Wang et al. 2004).

During the formation of sister chromatids or homologous chromosomes there exists a very accurate form of DNA repair called homologous recombination-mediated repair (HRR). HRR involves the repair of DNA double strand breaks by formation of Holiday junctions using template DNA from the undamaged homologous chromosome (Deans, Griffin et al. 2003). In addition to the genome surveillance role of HRR, other DNA repair mechanisms have evolved to mitigate DNA damage. These repair processes are referred to as DNA-PK dependant non-homologous end joining (D-NHEJ) and the backup-non-homologous end joining (B-NHEJ) resection pathway for resolving double stranded DNA breaks. While these aforementioned pathways resolve double strand breaks, single stranded DNA lesions utilize a unique repair mechanism (single stranded break repair - SSBR). Figure 4 shows a schematic of the three prominent DNA repair mechanisms and the key proteins that mediate each process. For the purpose of this

study the HRR pathway will not be included in the examination of contributing proteins since it requires template DNA strands that are not present in differentiating skeletal muscle cells that have exited the cell cycle.

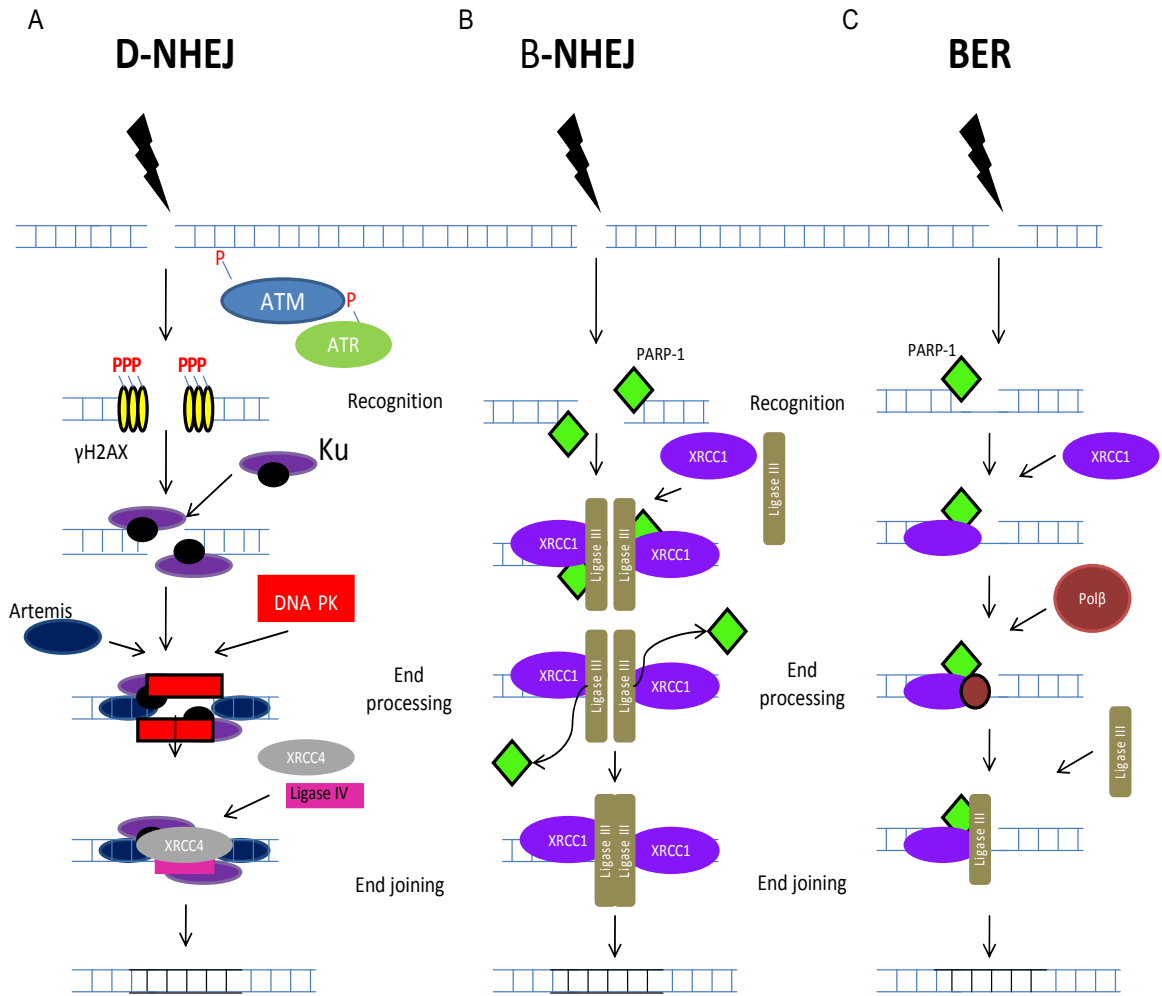


**Figure 4 Eukaryotic DNA repair mechanisms**

A) DNA PK dependant non-homologous end joining is a mechanism involved in the repair of double stranded DNA breaks. The histone H2AX at the site of damage is phosphorylated by ATM/ATR (ataxia telangiectasia mutated/ ataxia telangiectasia and Rad3-related proteins). Ku is then recruited to the site of damage by the presence of  $\gamma$ H2AX. Once bound to DNA, DNA PK (DNA dependent protein kinase) and Artemis are recruited next where they act to process the ends. DNA PK self phosphorylates to its active form DNA PKcs (DNA dependent protein kinase catalytic subunit) which recruits and activates further repair proteins such as DNA ligase IV and XRCC4 which are responsible for religating the broken ends. B) Backup non-homologous end joining requires PARP (poly (ADP-ribose) polymerase) to recognize the dsDNA lesion and recruit DNA ligase III and XRCC1 (X-ray repair cross complementing protein 1) to repair the break. C) Base excision repair (BER) is a mechanism for the repair of single stranded DNA lesions. It involves similar proteins to B-NHEJ including PARP to recognize the lesion and recruit further repair proteins. DNA ligase III and XRCC1 are recruited with PNK (polynucleotide kinase) and Pol $\beta$  (DNA polymerase beta) which process the ends of the lesion and fill in any gaps created by the repair process.

### **1.5.1 Repair of DNA double strand breaks**

Traditional non-homologous end joining (D-NHEJ) involves the repair of double stranded DNA breaks (ds) by direct joining of broken ends or by utilizing short segments of complimentary nucleotides in the event of end processing as outlined in the schematic in Figure 4 A (Frank, Sekiguchi et al. 1998). The occurrence of ds breaks are frequent in the normal life cycle of the cell as they can be induced by cellular processes or by exposure to ionizing radiation (Burma, Chen et al. 2006). In D-NHEJ the dsDNA break is detected by the Ku complex which consists of Ku70 and Ku80. DNA-PK then binds to the ds break specifically when Ku is bound and when in direct interaction with Ku leading to activation of the kinase. The catalytically active DNA-PK phosphorylates itself and other downstream targets to stabilize the repair complex and initiate the DNA repair process. For example, DNA-PKcs phosphorylates the protein Artemis, leading to activation of the protein as a 3' to 5' endonuclease capable of processing the broken ends of the DNA (Iliakis, Wang et al. 2004). Subsequently DNA-PKcs is released allowing the recruitment of other repair proteins to mend the lesion including DNA ligase IV and XRCC4. Often it is the case that a DNA polymerase is involved in aiding the ligation by filling in any gaps created by the damage event (Lieber, Ma et al. 2003).

The backup NHEJ pathway (B-NHEJ) is the most recently discovered pathway and is hypothesized to repair double stranded DNA strand breaks when the D-NHEJ pathway no longer functions (Audebert, Salles et al. 2004). The B-NHEJ pathway utilizes a separate complement of proteins to accomplish the same task as D-NHEJ (Figure 4B). In B-NHEJ PARP is the first protein recruited to the site of damage. It has been

hypothesized that histone H1 is not phosphorylated in responses to DNA damage by DNA PK as is the case in NHEJ. This lack of phosphorylation allows histone H1 to remain bound to the DNA to induce the recruitment and binding of PARP to the site of damage (Rosidi, Wang et al. 2008). PARP is responsible for the recruitment of DNA ligase III and XRCC1 which process and religate the broken strands. Not all of the details of this pathway have been elucidated, yet the prevailing hypothesis states that when activated the B-NHEJ pathway becomes the primary DNA repair response and permanently replaces the more rapid D-NHEJ pathway in the cell (Audebert, Salles et al. 2008).

### **1.5.2 The repair of single strand DNA lesions**

In addition to double strand breaks, the genome is also subject to single strand DNA nicks or gaps, often as a result of ionizing radiation or exposure to reactive oxygen species (Dianov and Parsons 2007). Interestingly, the single strand break repair (SSBR) pathway of base excision repair (BER) utilizes many components of the B-NHEJ pathway (Figure 4C). Here, there is an initial recruitment of PARP to the site of damage and then the subsequent recruitment of XRCC1 and DNA LigIII, to mediate end ligation. As the nature of the single strand break is fundamentally different than a double strand break, the ends must be further processed by polynucleotide kinase (PNK) to ensure that there is a 5' phosphate and 3' hydroxyl end. The gap that remains from this processing is filled by DNA polymerase  $\beta$  and then the nick is sealed by DNA LigIII (Almeida and Sobol 2007). The SSBR pathway is able to rapidly recognize and repair single strand breaks while the B-NHEJ pathway is not able to induce the repair of ds breaks as rapidly as the D-NHEJ pathway (Audebert, Salles et al. 2004).

The process of myogenesis involves an extensive genomic reprogramming in which many genes are up-regulated while a large number of gene products are silenced. Therefore it is reasonable to hypothesize that the global alteration in gene expression may be due, in part, to the lesions created by caspase 3/CAD during the initiation of differentiation. As such the subsequent repair of those lesions will be critical to complete the myogenic program and maintain genomic integrity.

## ***1.6 Hypothesis and Aims***

### **1.6.1 Hypothesis**

During skeletal muscle differentiation transient DNA lesions are formed that are required for the successful differentiation of myoblast muscle precursor cells into mature, multinucleated myotubes. It is therefore hypothesized that these transient lesions must be repaired by the cell via a known DNA repair pathway in order to avoid permanent nuclear damage.

### **1.6.2 Aims**

1. To further profile the formation and repair of transient DNA strand breaks observed during skeletal muscle differentiation.
2. To explore the contribution of DNA repair proteins from each of the candidate repair pathways in repairing the observed transient DNA strand breaks.
3. To examine the effects on muscle cell differentiation when candidate repair protein expression is perturbed in cultured cells.

## **2 Materials and Methods**

## ***2.1 Tissue culture***

### **2.1.1 C2C12 plating and passaging**

C2C12 murine myoblast cell line, ATCC, VA cell stocks stored at -80°C in growth media (Dulbecco's Modified Eagle Medium (DMEM), Gibco, NY with 10% fetal bovine serum (FBS), Gibco, NY and 2% PenStrep, Gibco, NY) containing 10% Dimethyl Sulphoxide (DMSO) Hybri-Max, Sigma, MO were thawed in a 37°C water bath. Cells were transferred to a 15mL conical tube containing 5mL of normal growth media and pelleted by centrifugation at 750xg for 5min. DMSO containing media was removed by aspiration and the cell pellet was resuspended in normal growth media. The resuspended cells were transferred to a 10cm tissue culture plate at a concentration of  $1 \times 10^6$  cells/plate in a total volume of 10mL per plate. The plate was rocked to ensure homogeneous cell dispersal. The cells were then incubated at 37°C with 5% CO<sub>2</sub>. The cells were allowed to grow to 80% confluence with the media being changed every 48hr. To avoid spontaneous differentiation C2C12 cells were passaged at 80% confluence. The media was removed and cultures were washed with 1x PBS. Next 1mL of Trypsin (0.25% Trypsin stock, Gibco, NY in 1xPBS with 100mM EDTA, pH 8.0) was added to the 10cm plate and rocked to ensure the entire surface was covered. The plate was incubated at 37°C for 5min and trypsinization was stopped by the addition of 5mL of normal growth media. The cells were removed to a 15mL conical tube and centrifuged at 750xg for 5min to pellet cells. The media was aspirated and the pellet was resuspended in fresh growth media. The cells were then re-plated to the required size tissue culture dish at the appropriate concentration.

To induce differentiation, C2C12 cultures were grown to confluence under normal growth conditions. Differentiation was induced by replacing the growth media with low serum differentiation media (DMEM containing 2% Horse serum (HS), Gibco, NY and 2% PenStrep). Cells were differentiated for the indicated times with the differentiation media being refreshed every 48 hours.

In order to induce UV damage in DNA damage control cells C2C12 cells were grown in normal growth media were exposed to 2 joules/m<sup>2</sup> UV radiation for 30 seconds then incubated at 37°C for 2hr before being collected as described.

To induce apoptosis, cells were grown in normal growth media and incubated with 1µM Actinomycin D, Sigma, MO for 18hr before being collected as described.

### **2.1.2 Primary Myoblast Isolation**

B6C3F1 mice were used to harvest primary myoblast from hind limb muscles. The mice were disinfected with 70% ethanol then the skin and fascia were removed to expose the hind limb muscles. The muscles were dissected and placed in a sterile 6cm plate. In a laminar flow hood the muscles were washed 2x in PBS (+2% PenStrep and 0.02% fungizone) making sure to remove all traces of hair and connective tissue. The clean muscle was transferred to a 10cm plate and cut with dissecting scissors until a pulp was obtained. The pulp was transferred to a sterile 15mL conical tube and washed 3x with 5mL supplemented PBS by inversion. The PBS was removed by aspiration and the 5mL of pre-warmed collagenase-dispase solution (dispase II, Roche and 1% collagenase (reconstituted in sterile PBS) with 2.5mM CaCl<sub>2</sub>) was added to the muscle pulp and incubated at 37°C for 45min with frequent inversion. The muscle was then

strained through a 40µm filter into a 50mL conical tube and washed 3 times with 5mL PBS. The slurry was centrifuged at 350xg for 15min. The supernatant was carefully aspirated so as not to aspirate the pellet. The muscle pellet was then resuspended in 10mL Ham's complete growth medium (Ham's medium, 20% FBS, 2% PenStrep, 0.6µg/mL fungizone and 2.5 µg/mL βFGF). The cells were pre-plated onto a non-collagen coated 10cm tissue culture dish and incubated at 37°C for 2hrs. The non-adhered cells and media were then transferred to a 10cm collagen coated plate (2mL of rat-tail collagen, Roche, NY containing 0.2% acetic acid was coated onto tissue culture plates) and incubated for 12hr at 37°C. Following the incubation the cell debris was removed and replaced with fresh complete growth media. The cells were maintained by replacing the media every 48hr. The cells were allowed to grow to 80% confluency before being passaged using trypsin.

Differentiation was induced in primary myoblast cells by replacing the complete growth media with primary differentiation media (DMEM containing 5% horse serum and 2% PenStrep). The media was changed every 24hr.

## ***2.2 Nucleic acid isolation and expression analysis***

### **2.2.1 RNA isolation from cultured cells**

C2C12 myoblasts were plated in 35mm plates, one for each experimental condition to be analyzed. The cells were allowed to grow to confluence after which time the cultures were either induced to differentiate using low serum media as described in section 2.1 or collected as growth condition cells. At the appropriate time point the cells were rinsed in 1X PBS. Next 250µL of TRIZOL reagent, Invitrogen, CA, was added to the

plate using RNase free pipette tips and swirled to ensure total coverage. The cells were incubated in TRIZOL for 5min at room temperature (RT). After incubation the plates were scraped using a cell lifter and the lysate was transferred to a 1.5mL RNase free microfuge tube. At this point the sample contained in TRIZOL was frozen at -80°C until such time that all the time points had been collected in TRIZOL. The TRIZOL lysates were then thawed on ice and 50µL of chloroform, molecular biology grade, Fisher, NJ was added to each sample. The samples were vortexed then allowed to incubate for 3min at RT after which time they were centrifuged at 10 000xg for 10min at 4°C to separate the phases. The top phase was removed to a fresh, labeled, RNase free tube while the organic layer was disposed of as waste. Next 125µL of isopropanol, Fisher, NJ was added to each sample and the tubes were gently inverted to mix. The tubes were rocked on a nutator for 20min at RT after which time the RNA was pelleted by centrifugation at 10 000xg for 15min at 4°C. The supernatant was discarded and the pellet was washed in 500µL 70% ethanol-DEPC (Ethanol, Fisher, NJ in Dimethyl Pyrocarbonate (DEPC), Sigma, NJ containing sterile water) and re-centrifuged for 5min at 7500xg at 4°C. The supernatant was discarded and the RNA pellet was allowed to air dry in the fume hood. Once dry the RNA pellet was resuspended in 50µL nuclease free water and allowed to dissolve at 4°C for 1hr before being stored at -20°C.

### **2.2.2 First strand cDNA synthesis**

In order to produce equal concentrations of cDNA for each sample the concentration of the RNA isolated from the cells was determined by UV spectrophotometry (1µL RNA in 99uL RNase free water). The samples were loaded into

a quartz cuvette and measured at an absorbance of 260nm. The samples were measured in duplicate and the average value was used to calculate the amount of RNA to be added to the first strand synthesis reaction. A minimum of 500ng of RNA in 10 $\mu$ L of RNase free water was used to generate the cDNA. To each sample 1 $\mu$ L of 0.5 $\mu$ g/ $\mu$ L Oligo(dT<sub>15</sub>) 12-18 Primer, Invitrogen, CA was added as well as 1 $\mu$ L of dNTP mix (10mM (each dNTP) PCR Nucleotide Mix (dNTP), Roche, IN). The samples were then incubated in a 65°C heat block for 5min. The tubes were removed to ice and centrifuged at 14000rpm using a bench top centrifuge. Next the samples were made up to 1X first strand buffer (5X first strand buffer, Invitrogen, CA), 10mM dithiothreitol (DTT), Invitrogen, CA and 2U/ $\mu$ L RNaseOUT Recombinant Ribonuclease Inhibitor, Invitrogen, CA was added to each tube. The samples were mixed and incubated at 42°C for 2min after which time 10U/ $\mu$ L Superscript II Reverse Transcriptase, Invitrogen, CA was added to each tube and then incubated at 42°C for 50min. The samples were heat inactivated at 70°C for 15min. Finally 2U/ $\mu$ L RNase H, Invitrogen, CA was added to each sample and incubated at 37°C for 20min.

### **2.2.3 Reverse Transcription Polymerase Chain Reaction (RT PCR)**

For each PCR reaction 0.5 $\mu$ g of cDNA product was used to be amplified. For each sample 0.125U/ $\mu$ L Taq DNA Polymerase Recombinant, Invitrogen, CA, 1X PCR Reaction Buffer, Invitrogen, CA, 250 $\mu$ M PCR Nucleotide Mix (dNTP), Roche, IN, 2mM magnesium chloride (MgCl<sub>2</sub>), Invitrogen, CA, 0.5 $\mu$ M forward primer and 0.5 $\mu$ M reverse primer was added in a master mix (for a complete list of primers used refer to Appendix Table 1). As a loading control PCR amplification was performed for the gene of interest and GAPDH

concurrently but in separate reaction tubes. Next 2 $\mu$ L of cDNA was added per PCR reaction and 18 $\mu$ L of the reaction mix was aliquoted per reaction in 200 $\mu$ L Thermowell tubes, flat cap (Corning, NY). The tube contents were mixed thoroughly and the tubes were placed in the PCR cycler (Eppendorf). The cycler was set according to the optimized PCR conditions and primer melting temperatures. A typical cycler setting was 95°C denaturation for 30sec followed by a 30sec annealing (temperature based on primer T<sub>m</sub>) and a 72°C extension for 45sec. For typical PCR amplifications 30 cycles were used. After the PCR amplification was complete, the DNA samples were separated on 1% agarose gel (1% w/v agarose LE in 100 $\mu$ L 1X TAE Buffer). The samples were prepared for electrophoresis by adding 1:10 10X DNA loading buffer to each. The samples were loaded into the prepared gel and electrophoresed at 100V until the dye front reached near the end of the gel. The gel was visualized using Alpha Imager UV light box (Alpha Innotech).

#### **2.2.4 Quantitative Real time RT PCR**

Quantitative RT PCR was conducted to measure the level of gene expression. Approximately 300 $\mu$ g cDNA was generated by SuperScript II reverse transcription and then added to 18 $\mu$ L of PCR master mix (2X QuantiFast SYBR Green PCR Master Mix, Qiagen, ON, Can) containing 5 $\mu$ M forward and reverse primers (each sample was run in duplicate). The gene of interest was amplified along with a GAPDH internal control for each sample condition. The samples were loaded into 100 $\mu$ L tubes (Corbett Research , Australia) held within a chilled metal block to ensure the samples were kept cold at all times. The sample tubes were loaded into a Qiagen RotoGene Q qPCR cycler and a two

step cycle was run with a 5min 95°C hot start activation step followed by 40 cycles of 10s denaturation at 95°C for 10sec and a combined annealing/extension step at 60°C for 30sec. After amplification the critical threshold (CT) was set to include the exponential growth curve of each sample. The delta delta CT was calculated by subtracting the CT of the gene of interest from the control and then by comparing the growth condition (normal condition) to the experimental condition (differentiation).

## ***2.3 Protein isolation and expression analysis***

### **2.3.1 Protein lysate collection and measurement of concentration**

Cells were cultured as described above and the plates were removed from the incubator at the appropriate condition/time point and placed on ice prior to protein collection. The cells were then rinsed with ice cold 1X PBS 3 times. The PBS was aspirated and 500µL of PLC gamma lysis buffer containing protease inhibitors was added (500µL per 10cm plate). This lysis buffer consisted of 50mM HEPES (pH 7.5), 150mM NaCl, 10% glycerol, Fisher, NJ, 1% TritonX-100, Sigma Aldrich, MO, 1mM EGTA, 1.5mM MgCl<sub>2</sub>, 20mM NaF, 10mM Na Pyrophosphate, and 1% of each protease inhibitor just prior to use (PMSF(1mg/mL), Aprotinin (1mg/mL), Pepstatin (1mg/mL) Leupeptin (1mg/mL) and NaV (0.5M)). The plates were kept on ice and incubated for 30-45min on a rocker, then scraped to collect the lysate. The lysate solution was transferred to a pre-labeled microfuge tube and placed on ice. The tubes were centrifuged to remove cellular debris at 14 000xg for 5min at 4°C. The supernatant was collected and the pellet was discarded. The lysates were stored at -80°C until such time that the concentration was measured. To measure protein concentration a standard curve was generated by

preparing standards of known concentrations at 0, 1, 3, 5, 7 and 10 µg/ml Bovine Serum Albumin (BSA), Roche in dH<sub>2</sub>O. Subsequently, 1µL of each experimental sample was added to 799µL of dH<sub>2</sub>O. To each sample 200µL of Bio-Rad protein assay dye reagent concentrate, Bio-Rad, CA was added and the samples were mixed thoroughly and transferred to disposable cuvettes. The sample absorbance was measured using a spectrophotometer set to visible light at a fixed wavelength 595nm to obtain the sample concentration.

### **2.3.2 Western Blot Analysis of Protein Expression**

Indicated amounts of protein lysates were prepared for separation on a 10% SDS PAGE gel by addition of 1:5 5X Laemmli buffer to the protein lysate and boiling at 100°C for 5min. The samples were loaded into the prepared gel (10% 4X Stacking Buffer (for 100mL volume: 6g Tris Base, 0.4g SDS, dH<sub>2</sub>O to 100mL, pH 6.8 with HCl) 5%, 4X Separating Buffer (for 250mL volume: 0.18g/mL Tris Base, 4mg/mL SDS, dH<sub>2</sub>O to 250mL, pH 8.8 with HCl) along with BenchMark protein ladder. The gel was run in a Hoefer electrophoresis apparatus at 100V in 5X Running Buffer (15g/L Tris Base, 72g/L Glycine, 5g/L SDS in dH<sub>2</sub>O) until the dye front reached the end of the gel. Once electrophoresis was complete the gel was removed from the apparatus and the protein was transferred to a nitrocellulose membrane that had been pre-wet with Transfer Buffer ( 7.3mg/mL Tris Base, 9.8mg/mL glycine, 0.04% SDS, 2.5% Methanol) using semi-dry transfer apparatus at 9V for 2hr. After transfer, the membrane was allowed to air dry and was re-wet with methanol. The wet membrane was rinsed in TBST and blocked for 1hr in blocking solution (5% Powdered Skim Milk in 0.1% TBST) on a rocker. The

blocked membrane was probed using a primary antibody (DNA ligase IV (H-300) rabbit polyclonal IgG (200µg/mL), Santa Cruz Biotechnology, CA 1:500, Anti-XRCC1 antibody produced in rabbit (1mg/mL), Sigma-Aldrich, MO 1:500 or Anti-tubulin (E7), mouse monoclonal, Developmental Studies Hybridoma Bank, University of Iowa, IA) 1:100) for 24hr at 4°C. After probing the membrane was washed 3X in TBST. After washing the membrane was incubated in secondary antibody (Goat Anti-Mouse IgG (H+L)-HRP Conjugate, Bio-Rad, CA 1:5000 or Goat Anti-rabbit IgG (H+L)-HRP Conjugate, Bio-Rad, CA 1:5000) at the described concentration for 1hr at RT. The membrane was again rinsed and was then developed using SuperSignal West Pico Chemiluminescent Substrate, Thermo Scientific, IL (50% SuperSignal West Pico Luminol/Enhancer and 50% SuperSignal West Pico Stable Peroxide Solution) incubated for 5min at RT. The chemiluminescent reaction was visualized either using Alpha Innotech FluorChem HD2 or by exposure to Kodak film, subsequent analysis was performed by Alpha View software or Image J respectively.

#### ***2.4 Single cell gel electrophoresis***

Primary myoblast or C2C12 myoblast cells were grown on a 10cm tissue culture plate, treated as indicated (*ie.* induced to differentiate, caspase 3 inhibited, etc), collected in freezing media and frozen at -80°C. For the comet assay the cells were thawed in 37°C water bath and transferred to growth media. The thawed cells were then centrifuged at 720xg for 5min. The media was then removed and the cells were resuspended in ice cold 1X PBS. At this point the cells were ready to proceed with the comet assay using the Comet Assay Reagent kit for Single Cell Gel Electrophoresis,

Trevigen, MD. In preparation for the comet assay the Lysis Solution (included in kit) was chilled on ice for at least 20min prior to use. Next the low melting-point agarose (LMA) was melted by submerging in a beaker of boiling water for 5min with the cap loosened. The agarose was maintained in a liquid state by transferring to a 37°C water bath. The LMA was allowed to cool at 37°C for at least 20min prior to use. Cell samples, at a concentration of  $1 \times 10^5$  cells/mL, were combined with LMA at a ratio of 1:10 cells:LMA and immediately pipetted onto labeled Gelbond film strip (agarose gel support medium) Lonza, ME in 75 $\mu$ L aliquots. Cells were applied to the hydrophilic side of the film to ensure that the sample spread evenly into a circle of approximately 25mm in diameter. Each film was placed flat at 4°C in the dark for 10min or until the gel solidified. The slide was then immersed in pre-chilled lysis solution and incubated at 4°C for 45min. After incubation the lysis solution was removed and the slide was immersed in freshly prepared Alkaline Solution pH>13 (6g NaOH, 250 $\mu$ L 200mM EDTA, dH<sub>2</sub>O) for 45min in the dark. The slide was removed from the alkaline solution and transferred to a horizontal electrophoresis apparatus where it was placed equidistant from each electrode in alkaline electrophoresis solution (12g/L NaOH, 1mM EDTA pH8). Temperature fluctuations were minimized in the non-buffered system by running the electrophoresis at 4°C in walk in refrigerator. The voltage was set to 30V for 30min at constant amperage of 300mA. Following electrophoresis the slide was rinsed several times in dH<sub>2</sub>O then immersed in 70% ethanol to fix. Next the slide was dried in an air tight container containing desiccant overnight at room temperature. Once dry, the slide was stained by submerging in SYBR Green stain at 1:10000 in TE buffer pH 7.5 for 5min.

The slide was then removed and allowed to air dry. The dry slides were mounted with coverslips and the cells were visualized by fluorescence microscopy using the GFP channel (494nm) at 20x magnification.

## **2.5 *In situ* nick translation**

C2C12 mouse myoblasts were plated onto UV irradiated glass cover slips in 35mm tissue culture dishes at a concentration of  $0.5 \times 10^6$  cells/plate. One plate was prepared for each experimental condition, plus one DNaseI positive control plate for each experimental parameter. The cells were allowed to grow to confluence in a 37°C incubator. Prior to initiating the *in situ* nick translation assay the 10X ISNT reaction buffer (0.5M TRIS-HCl pH 7.9, 50mM MgCl<sub>2</sub>, 100mM β mercaptoethanol) and ISNT reaction mix (1X ISNT reaction buffer, 10μM dNTP (1mM dCTP, dATP, and dGTP), 1μM dTTP, 1μM digoxigenin (DIG)-II-dUTP, 0.1% DNA Polymerase I, New England Biolabs) were prepared. Positive control plates were washed in 1X PBS. Next the cover slips were treated with 200μL of DNaseI treatment mix (1% DNaseI, 1X DNase Buffer) and incubated for 10min at room temperature (RT). After incubation the cover slips were washed 2 times in 1X PBS. The DNaseI and experimental condition cover slips were all rinsed with 1X ISNT reaction buffer (made by diluting the 10X reaction buffer 1:10). After rinsing each cover slip was incubated with 200μL of ISNT reaction mix and incubated at 37°C for 45min with gentle agitation. After 45min the cover slips were washed 2 times in 1X PBS then immuno-stained as described in Section 2.8 using a mouse anti-DIG primary antibody at a concentration of 1:500 in 3% BSA for 1hr at RT.

## **2.6 *shRNA mediated knock down of XRCC1***

Target sequences of shRNA were cloned into the appropriate vector (TRC mouse shRNA individual clone lentiviral pLKO.1 targeted to XRCC1, Open Biosystems/Thermo Scientific, AL, pCMV-dsRed-Express Vector, Clontech, CA or nonsilencing pGIPZ (shNEG), Open Biosystems/Thermo Scientific, CA) and the plasmid DNA was amplified by culturing the *E. coli* engineered to express each plasmid in antibiotic media containing either Ampicillin or Kanamycin (40µg/mL in LB broth). After colony expansion the bacterial plasmid DNA was purified using HiSpeed Plasmid Midi Kit (25), Qiagen, ML. The purified plasmid DNA was verified for size by performing a restriction digest using the restriction enzymes Bam HI and ClaI. The digests were separated on 1% agarose gels (plus 0.1µg/mL EtBr) to check that the DNA fragments were of the appropriate size as predicted from the restriction map for the plasmid of interest.

One day before transfection C2C12 myoblast cells were cultured in 35mm tissue culture plates in PenStrep free growth media to a confluence of 50-60%. The cells were rinsed with 1X Opti-Mem I reduced serum media, Gibco prior to transfection. The shRNA was prepared by diluting 16µg/mL DNA per condition in Opti-Mem. Similarly, the Lipofectamine 2000 was diluted to 4% in Opti-Mem. The solutions were allowed to incubate for 5min at room temperature. The Lipofectamine 2000 solution was then mixed into the shRNA solution and gently mixed. The Lipofectamine-shRNA solution was allowed to incubate for 20min at RT. Next 500µL of the transfection solution was added to each plate and incubated at 37°C for 3hr. After incubation 1mL of antibiotic free growth media was added to each plate and the cells were incubated for a further 12-

18hr. At this point cell cultures were either induced to differentiate using low serum media or collected for growth condition.

### ***2.7 Inhibition of caspase 3***

Cultured myoblasts were pre-treated with either 15 $\mu$ M z.DEVD-FMK (DEVD), Bio Vision or 15 $\mu$ M Dimethyl Sulphoxide (DMSO) Mybri-Max, Sigma, MO for 2hr at 37°C. After pre-treatment the cells were induced to differentiate using low serum media or continued in growth media both containing 15 $\mu$ M DEVD or DMSO as a vehicle only control. The inhibition or control media was changed every 48hr until the end of the time course. The cells were collected at the appropriate time points/treatments and analyzed as described.

### ***2.8 Immunofluorescent staining***

Cells were cultured on 25mm coverslips in 35mm plates and exposed to the described experimental conditions. At appropriate time points the cell plates were removed to ice and the media was aspirated and replaced with ice cold 1XPBS. The plates were washed a further 2 times with PBS. The cells were fixed in 90% methanol for 8min on ice. The fixative was removed and the cells were washed with PBS 2 times. Next the cells were covered with PBS and the plates were wrapped with Parafilm and stored at 4°C until such time that all time points had been fixed. The plates were removed to RT and blocked for 24hr in 3% FBS. After blocking the cells were incubated in primary antibody (DNA ligase IV (H-300) rabbit polyclonal IgG (200 $\mu$ g/mL), Santa Cruz Biotechnology, CA 1:00, Anti-XRCC1 antibody produced in rabbit (1mg/mL), Sigma-Aldrich, MO 1:100, Anti-Myosin Heavy Chain (MF-20) mouse IgG, Developmental Studies

Hybridoma Bank, IO 1:50) made up in blocking solution for 24hr at 4°C. After primary antibody incubation the cells were washed 3 times in PBS and incubated in secondary antibody (2mg/mL Alexa Fluor 488 goat anti-rabbit IgG (H+L), Invitrogen, CA 1:500, 2mg/mL Alexa Fluor 594 goat anti-rabbit IgG (H+L), Invitrogen, CA 1:500, 2mg/mL Alexa Fluor 594 goat anti-mouse IgG (H+L), Invitrogen, CA 1:500, AP129F Donkey anti-mouse IgG FLUOR, Chemicon International, CA 1:500) diluted in PBS for 1hr (RT) to 24hrs (4°C). After incubation the cells were washed 2X in PBS and 1X in dH<sub>2</sub>O then counterstained with DNA specific 4',6-Diamidino-2-phenylindole dihydrochloride (DAPI), Sigma Aldrich, MO made up in dH<sub>2</sub>O (1:10 000) for 10min at RT. After incubation the cells were washed 2 times in PBS and 1 time in dH<sub>2</sub>O. The coverslips were mounted on microscope slides using Dako Fluorescent Mounting Medium and visualized using a Zeiss Observer.Z1 inverted fluorescence microscope.

### **3 Results**

### ***3.1 Temporal location of DNA damage in skeletal muscle differentiation***

Prior observations from our laboratory have shown that DNA damage occurs during skeletal muscle differentiation (Larsen et al. 2010). Multiple methods were employed to demonstrate that DNA lesions were observed during early stages of myoblast differentiation, lesions that subsequently disappeared at later time points. Two methods that were used included immunofluorescent staining for the histone variant  $\gamma$ H2AX which is phosphorylated upon detection of DNA damage within the cell as well as *in situ* nick translation which uses DNA polymerase I to insert a labeled nucleotide (DIG II dUTP) wherever a DNA lesion occurs within the DNA. These initial experiments revealed that DNA lesions appeared 12 to 24 hours after the cells had been induced to differentiate using low serum media (Larsen, Rampalli et al. 2010).

In addition to this analysis, a single cell gel electrophoresis assay (commonly referred to as the comet assay) was performed to examine the extent of the DNA damage. The comet assay was performed by embedding myoblast cells in low melting point agarose, before lysing the cells with the appropriate buffer. Following lysis the embedded cells were incubated in an alkaline solution to ensure that the DNA was denatured to a single stranded form, allowing for better migration of the DNA when electrophoresed. The cells were electrophoresed in an alkaline running buffer and stained with SYBR green which is specific to DNA. The resulting comets were monitored for the extent of migration of the DNA from the nucleus. Based on the properties of electrophoresis, smaller fragments of DNA migrate further and the greater the number of fragments is directly proportional the extent of fragmentation or DNA damage. The

assay was performed in both mouse primary myoblast cells and in C2C12 cells (an immortalized myoblast cell line taken from mice). The results observed in the two cell types were similar, with DNA damage observed early in a differentiation time course, with a reduction in detectable DNA damage at later time points. In primary myoblasts, the earlier onset of the appearance of DNA lesions is likely due to a difference in the differentiation times between the two cell types. Here, the peak of DNA fragmentation was observed at the 12hr time point while in C2C12 myoblasts the peak of DNA fragmentation was noted at 24hr post low serum induction of differentiation as represented in Figure 5. The comet assay was used as both a qualitative and quantitative assay. In Figure 5 panel A, representative cells were selected to highlight the length of the comet tails observed for that particular condition.

A noteworthy observation (or caveat) from the comet assay was that in some cases the growth condition comets had rather lengthy tails. This is likely due to the amount of small DNA fragments that are sometimes present in a proliferating cell. These cells are still cycling normally and as such are undergoing mitosis and DNA replication as well as the common insults that a cell has to deal with in normal growth conditions. In addition, Trevigen, the manufacturer of the comet assay kit has reported that ambient light can also cause some DNA damage in the pre lysed cells. Despite these potential confounding issues, large concentrations of DNA were never observed near the nucleus in proliferating cells. For example, the nuclei/DNA of growing myoblasts were typically concentrated with smaller amounts of DNA extended into a comet tail. Given that DNA damage in a differentiating myoblast is transient, then the damage event itself is most

likely associated with targeted strand breaks and formation of very large fragments rather than the fragmentation pattern observed during apoptosis with the formation of small DNA segments. As such, we monitored the distance of migration for these dense DNA concentrations relative to the center of the nuclei. Each time point was represented graphically in Figure 5 panel B. In addition, the distance of migration was normalized to the growth conditions for both primary myoblasts and C2C12 myoblasts.

The results indicated that DNA lesions were most extensive early in the differentiation timecourse for both primary and C2C12 myoblasts (12hr for primary myoblasts and 24 hr for C2C12 myoblasts;  $P < 0.05$  and  $P < 0.01$  respectively). These results are similar to those previously reported (Larsen et al. 2010). As a positive control, myoblasts were exposed to an apoptosis inducing agent Actinomycin D and were collected 2hr post treatment. The migration of the DNA in this condition suggests that the DNA has been fragmented into a very small size, allowing for extended migration from the nuclei (see above). This qualitatively different appearance is dramatically different from that observed with differentiating myoblasts. In the latter case, there is no massive degradation of the DNA.

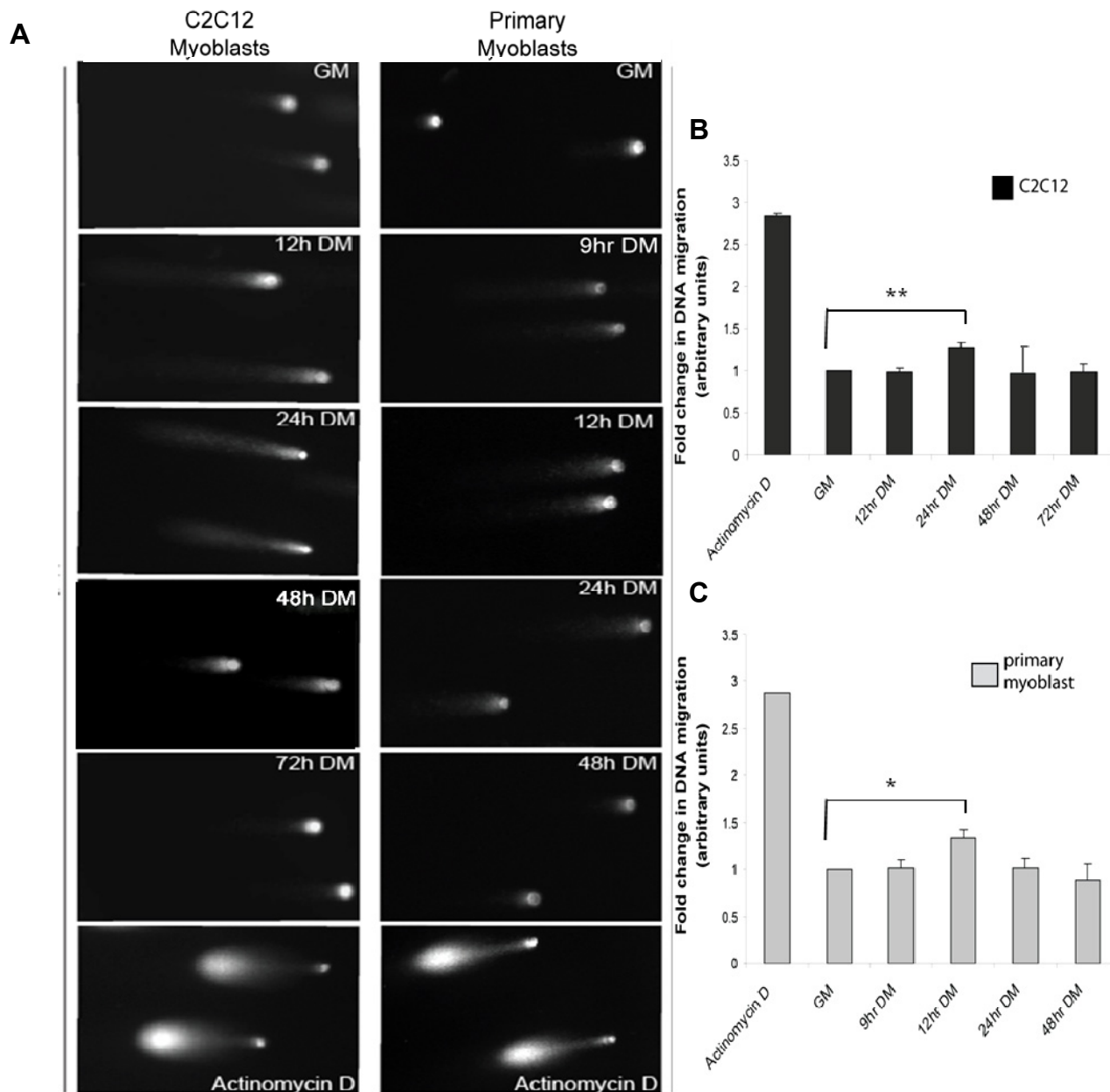


**Figure 5 Single cell gel electrophoresis in primary myoblast and C2C12 myoblast cells over the differentiation time course reveals the temporal location of transient DNA lesions.**

Single cell gel electrophoresis or Comet assay was performed in both primary myoblast cells and in C2C12 myoblast cells. The cells were cultured and induced to differentiate in low serum media before being collected in frozen stocks. The apoptosis control cells were exposed to 1.0uM Actinomycin D before collection. A) After electrophoresis the cells were stained with SYBR green fluorescent dye specific to nucleic acids. The comets were visualized under 20X magnification using a fluorescence microscope. B, C) The length of migration of the concentrated DNA within each tail was measured using image j software and the relative lengths were normalized to growth. The fold change in length compared to growth conditions were plotted from the results of n=3 experimental trials consisting of 100+ comets per trial. The starred columns represent a statistically significant difference between the time points as determined using student t two tailed statistical analysis where  $p < 0.05$ .

### ***3.2 Expression of DNA repair proteins during differentiation of skeletal myoblasts***

The observation that DNA lesions were present during early stages of myoblast differentiation and not at later time points indicated that an active DNA repair process may have been engaged. Indeed, the viability of a long lived cell type such as a muscle cell would require repair of the DNA damage accrued during differentiation. Here, we investigated the expression of candidate proteins from different DNA repair mechanisms in an effort to elucidate the operative DNA repair pathway. First, RT PCR was performed to measure the expression of a variety of DNA repair factors; these included DNA ligase IV, XRCC1, DNA PKcs, Gadd45a, PARP1 and XRCC6 (Ku70). The amplification products were separated on 1% agarose gels and visualized under UV light. Most of these gene products displayed similar expression patterns, with a decrease in expression at 12hr post low serum induction of differentiation and a subsequent up regulation in expression at 24hr post low serum induction (Figure 6). Of interest, the expression level of these factors generally declined at later stages of myoblast differentiation.

Given the phasic expression pattern, we next measured whether these repair factors exhibited any alteration in subcellular localization that may have coincided with repair of discrete damage foci. Here, candidate proteins were chosen from each major DNA repair process including DNA ligase IV which is typically involved in the NHEJ pathway; 53BP1 which is involved in double strand break repair; and XRCC1 which is typically implicated in BER in single strand break repair or, less commonly, in the backup version of NHEJ. In the case of DNA ligase IV and 53BP1, both proteins were present in

myoblast nuclei, yet neither of these factors exhibited any change in localization following low serum induction of differentiation (Figure 7). It was previously observed that ATM, a repair protein implicated in the recognition of double strand breaks, showed no change in localization early in differentiation in correlation with the observations seen with DNA lig4 and 53BP1 as shown in Appendix Figure S. 2. However, treatment with known DNA damaging agents (UV and Neocarzinostatin) induced clear foci formation in myoblasts, suggesting that these factors participate in the DNA repair process in response to exogenous insults.

Despite the lack of visible nuclear foci for DNA lig 4 and 53BP1, XRCC1 displayed dramatic foci formation during myoblast differentiation. Punctate nuclear foci appeared early in the differentiation time course and subsequently disappeared in later time points (Figure 8). The presence of these foci was not observed in proliferating C2C12 myoblasts, although formation of punctate nuclear foci was noted following UV irradiation (Figure 8 panel A). To quantify the formation of XRCC1 foci images were taken of 5 fields of view for each slide for 3 separate experiments (the number of cells counted per experimental repeat was in excess of 100 cells). The total number of foci per nucleus was counted and averaged, as represented graphically in panel B of Figure 8. Accordingly, formation of XRCC1 foci was most abundant at 24hr post differentiation, with an almost 2 fold greater number of foci compared to growth conditions ( $P < 0.01$ ; ANOVA).

In addition to monitoring foci formation, total protein content was also measured for both XRCC1 and DNA ligase IV. Western blot analysis was performed and

the relative band intensities of both anti-XRCC1 and anti-DNA lig4 protein blots were compared to a loading control ( $\beta$ tubulin) for each time point. The band intensities/quantification were measured using image j software and normalized to the loading control as described in Figure 9 A and B.

The results indicate that there is change in the expression patterns of both DNA lig4 and XRCC1, but the change in XRCC1 expression appears to be greater over the time course. Message levels for both DNA lig4 and XRCC1 were also examined over the same time course using real time RT PCR analysis and then values were normalized to the growth condition to obtain a  $\Delta\Delta$ ct value (which was plotted in Figure 9 panel C). These results were similar to the original RT PCR results, indicating that no significant change in gene expression was observed for XRCC1. Interestingly, the expression of DNA lig4 varied over the differentiation time course compared to XRCC1. However, this variation in DNA lig4 message content was not significant owing to the variability of the expression data ( $P>0.05$ ). The data presented here suggests that DNA repair proteins are present in myoblasts at similar concentrations, yet only XRCC1 displayed dynamic reorganization during a differentiation time course. Given these observations, XRCC1 was chosen for further analysis.

Next, we examined whether the formation of XRCC1 foci and the formation of DNA lesions were observed concurrently during myoblast differentiation. XRCC1 was monitored via immunocytochemistry using an anti-XRCC1 antibody, while DNA lesions were monitored using *in situ* nick translation staining for DNA damage. We did not find any notable degree of co-localization at either 24 or 48 hours post low serum induction

of differentiation (Figure 10), however there was detectable overlap at 12 hours post low serum induction. This general lack of overlap in XRCC1 and ISNT detected foci suggested that the DNA damage and DNA repair events were sequential rather than parallel or simultaneous. Accordingly the localization of the XRCC1 protein would indicate that the DNA lesions are being subject to active repair once DNA damage has subsided. Interestingly, the ISNT staining pattern was most prevalent in the euchromatin region of the nucleus suggesting that the DNA damage was concentrated in actively transcribed regions of the genome.

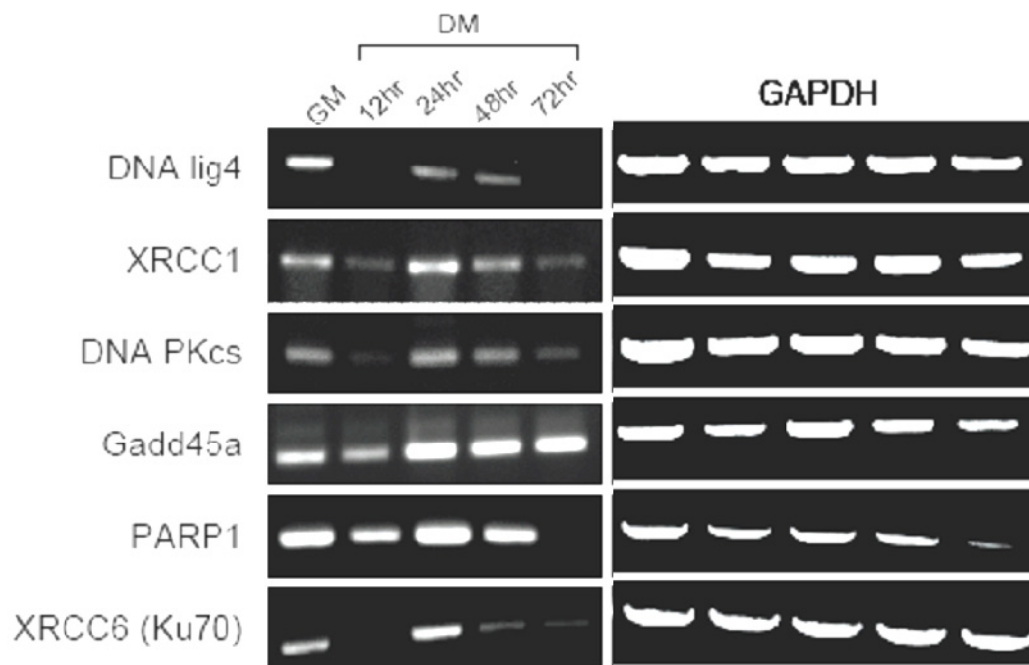


**Figure 6 RT PCR gene expression analysis of DNA repair protein candidates in differentiating C2C12 cells.** The cells were induced to differentiate using low serum media and the total RNA was isolated. The RNA was reverse transcribed to cDNA and RT PCR amplified using primers specific to the gene of interest and GAPDH as an internal loading control. The PCR product was separated on a 1% agarose gel containing ethidium bromide and viewed under UV light to visualize the DNA bands. n=3

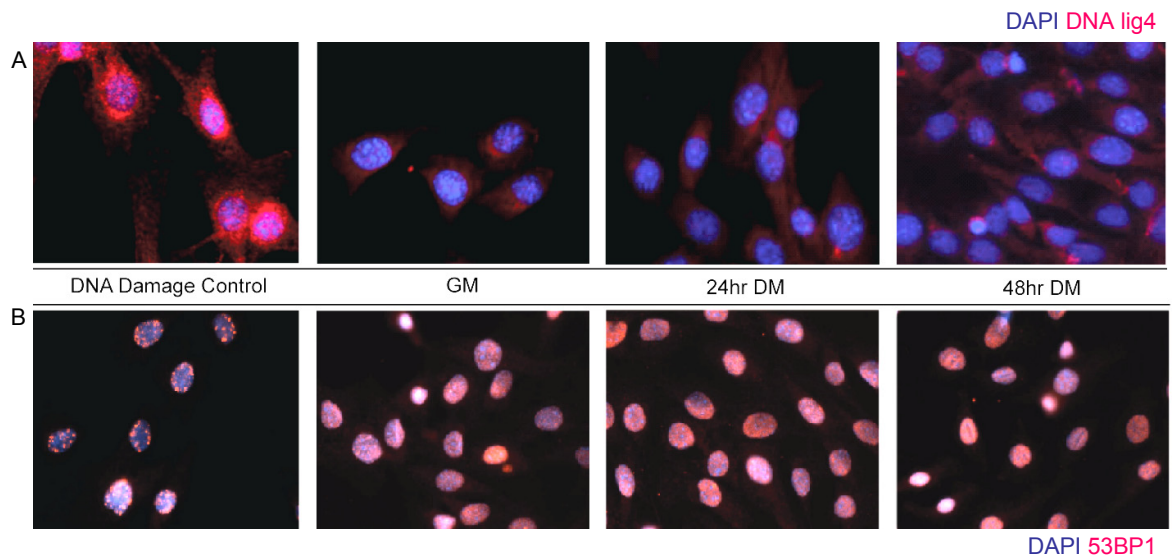


**Figure 7 DNA ligase IV and 53BP1 immunofluorescent staining in C2C12 myoblast cells does not reveal a change in protein localization following induction of differentiation.**

Proliferating C2C12 cells were induced to differentiate using low serum media for the indicated time period and were then fixed in 90% methanol or were fixed in growth media. A) The control cells were left in growth media and were exposed to 30 sec of UV radiation after which time the cells were incubated for 2hr before fixing. The fixed cells were immunofluorescently stained for DNA lig4 using anti-DNA lig4 primary antibody (1:100) and anti-rabbit Alexa594 conjugated secondary antibody (1:500). The cells were counter stained with DAPI (1:10000). The cells were visualized at 20X magnification using a fluorescent microscope. B) The control cells were incubated with 1uM Neocarzinostatin for 18hr to induce DNA damage and fixed. The cells were stained with an anti-53BP1 primary antibody (1:100) and stained as in A. n=3

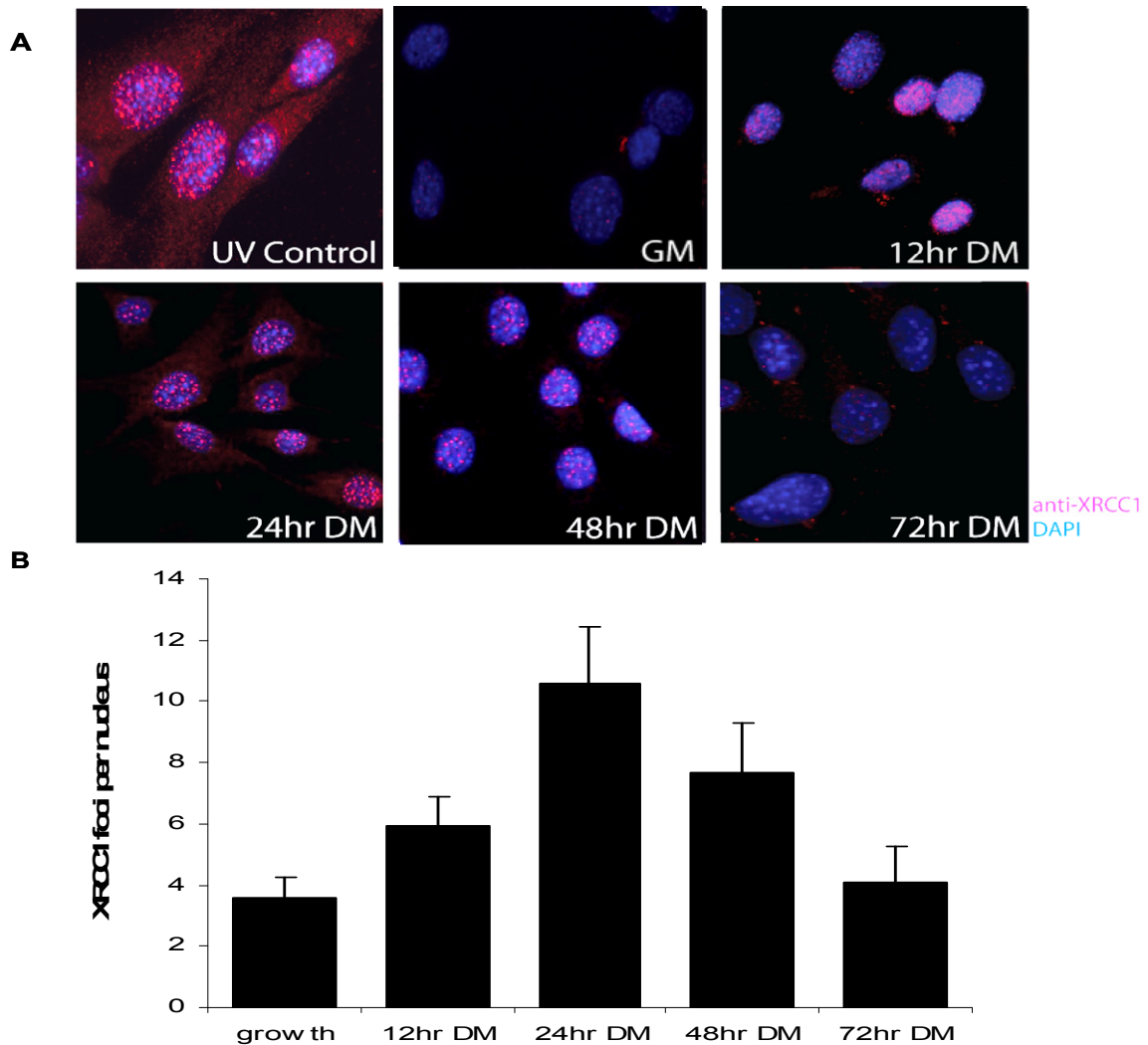


**Figure 8 XRCC1 forms distinct nuclear foci early in skeletal muscle differentiation in C2C12 cells upon low serum induction of differentiation.**

Proliferating C2C12 cells were methanol fixed or induced to differentiate using low serum media and fixed at the indicated time point. The fixed cells were immunofluorescently stained for XRCC1 using anti-XRCC1 primary antibody (1:100) and anti-rabbit Alexa594 secondary antibody (1:500). The cells were counter stained with DAPI nuclear specific stain (1:10000). A) The cells were visualized at 60X magnification using a fluorescence microscope, representative images presented. B) The cells from 5 fields of view from each time point were counted for number of XRCC1 foci formed and this was repeated to n=3. The average number of foci per nucleus is represented graphically. The data was found to be statistically significant by ANOVA  $p < 0.01$

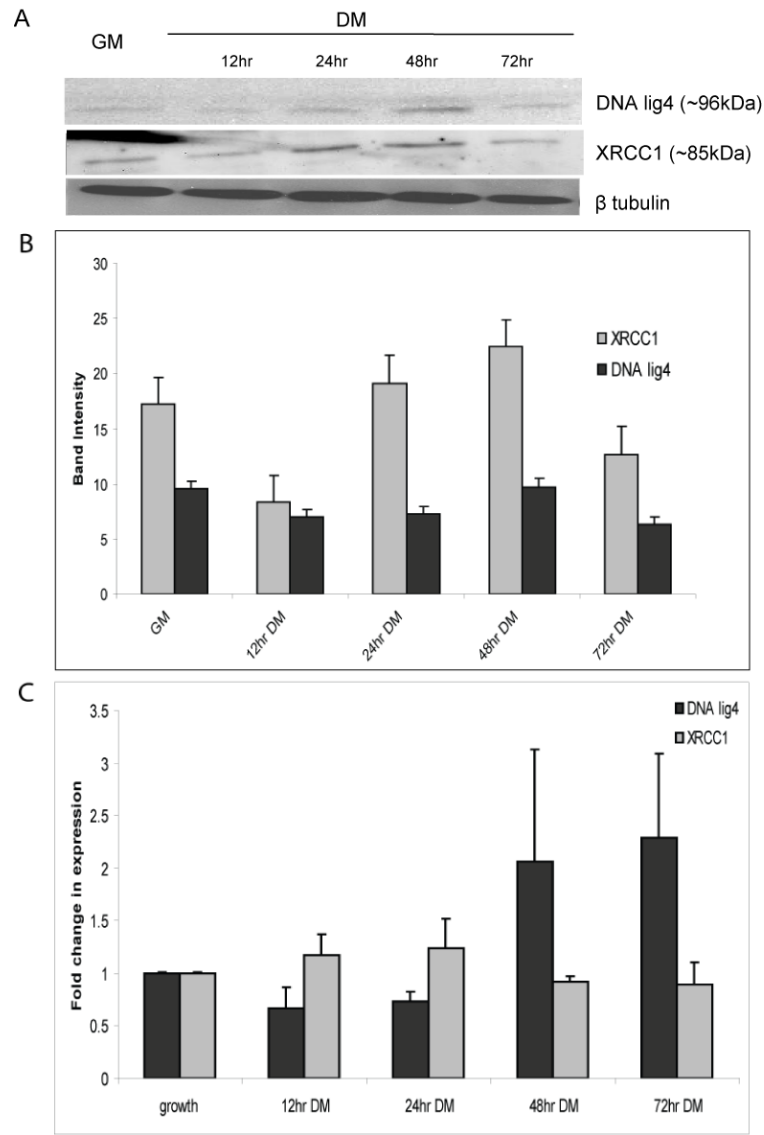


**Figure 9 Protein and gene expression of XRCC1 and DNA ligase IV in differentiating C2C12 myoblast cells.**

A) Western blot analysis of protein lysates collected from proliferating C2C12 cells or low serum induced differentiating cells. 50ug of protein was loaded and separated on a 10% SDS PAGE gel. The protein was transferred to a nitrocellulose membrane and probed for either XRCC1 using anti-XRCC1 primary antibody (1:500) or DNA lig4 using anti-lig4 primary antibody (1:500). A secondary anti-rabbit HRP conjugate was used to visualize protein bands (1:5000) using the WestPico system. B) The relative band intensity was measured using image j software and normalized to the Tubulin loading control band intensities. The data from n=4 blots was used to plot an average protein expression for each protein. C) The gene expression of both XRCC1 and DNA lig4 was determined using real time RT PCR. The RNA was isolated from C2C12 cells and reverse transcribed to cDNA using SuperScript II. The cDNA was qPCR amplified and normalized to a GAPDH internal control. The normalized expression was then normalized to the growth condition ( $\Delta\Delta ct$ ). The average expression from n=3 experimental procedures is represented.

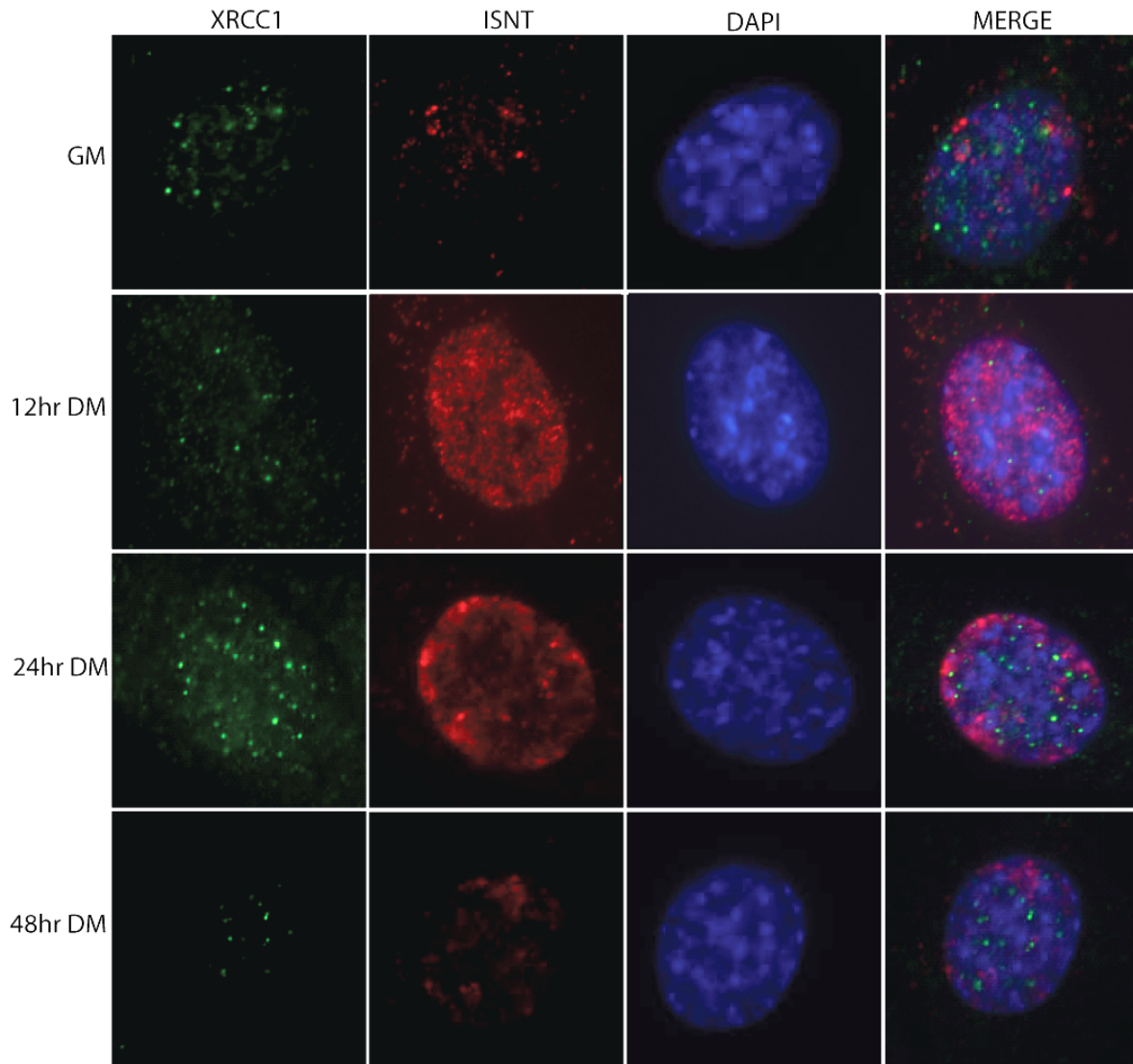


**Figure 10 Co staining for XRCC1 foci formation and *in situ* nick translation assay in C2C12 myoblast cells over differentiation reveals that XRCC1 foci form following DNA damage.**

ISNT was performed on 90% methanol fixed proliferating cells or in cells induced to differentiate using low serum media. As a positive control proliferating cells were exposed to DNase I prior to the ISNT assay to reveal robust incorporation of DIG dUTP indicated by intense staining (not pictured). All cells were incubated in anti-DIG dUTP (1:500) where the newly incorporated dUTP nucleotides were labeled with the DIG antibody. The cells were then co-stained for XRCC1 using antiXRCC1 primary antibody (1:100). A secondary antibody mix was used to fluorescently label the DIG antibody with an Alexa594 fluorescent tag and the XRCC1 with an Alexa488 green fluorescent tag (both 1:500). The cells were counter stained with DAPI a specific DNA stain. The cells were visualized under 60X magnification using a fluorescence microscope.

### ***3.3 The effect of caspase 3 inhibition on XRCC1 foci formation during myoblast differentiation***

Caspase 3 plays a crucial role in skeletal muscle differentiation as evidenced by the marked reduced ability of caspase null myoblasts to form multinucleated myotubes (Fernando, Kelly et al. 2002);(Larsen, Rampalli et al. 2010). A similar observation was noted when caspase 3 was chemically inhibited in C2C12 myoblast cells using z.DEVD.fmk (Fernando, Kelly et al. 2002). The peptide inhibitor z.DEVD.fmk functions by binding to the active site of the protease using the specific DEVD amino acid sequence (aspartic acid, glutamic acid, valine, aspartic acid). The reaction is made irreversible by the addition of a fluoromethyl ketone group (FMK), a side chain that confers no cytotoxic effects to the cells. The addition of a benzyloxycarbonyl group (z) to the N-terminal end of the inhibitor for enhanced cell permeability. When caspase 3 was inhibited (via treatment with the peptide inhibitor) in differentiating C2C12 myoblasts there was a significant reduction in the number of XRCC1 nuclear foci compared to DMSO treated control myoblasts (Figure 11). Although XRCC1 expression was detectable in caspase 3 inhibited myoblasts, there was no formation of punctate XRCC1 foci when compared to the DMSO control.

In addition to monitoring XRCC1 foci alone, the formation of strand breaks and the XRCC1 foci were simultaneously measured in C2C12 myoblasts. The images in Figure 12 revealed that there is a block in the formation of DNA strand breaks (as indicated by a lack of DIGII staining) with a similar loss in the formation of XRCC1 foci. XRCC1 foci formation was quantified by performing counts for each time point in the caspase 3

inhibited condition as well as in the DMSO vehicle only control condition. When caspase 3 was inhibited we noted a significant decrease in the number of XRCC1 foci formed ( $P < 0.05$ ; Figure 12B). Figure 12 B shows that the formation of foci in the DMSO treated cells follows a similar pattern as previously observed in untreated C2C12 myoblasts, in that the majority of the foci are seen at the 24hr time point and then are not detectable at later stages. In the caspase 3 inhibited myoblasts the increase in foci formation and the amount of foci observed per nucleus was significantly reduced compared to DMSO treated myoblasts ( $p < 0.01$ ). Indeed, the XRCC1 foci formation in caspase inhibited myoblasts was similar to the limited foci formation observed during growth conditions.

A second experimental procedure was employed to determine the effect of caspase 3 inhibition on the formation of strand breaks over the differentiation time course in myoblast cells. Here, we utilized the comet assay to document DNA damage events in both primary myoblasts and in C2C12 myoblasts. In both cell types caspase 3 was chemically inhibited using z.DEVD.fmk as in the immunocytochemistry experiments above. In caspase 3 treated myoblasts the DNA appeared to remain in the nucleus and to migrate a very limited distance, while in the DMSO treated cells the concentrated DNA migrated out from the nucleus in a pattern that was similar to our previous observations (Figure 13). In panel B, the results of the comet length measurements reveal that C2C12 myoblasts display a significant variation in comet length ( $p < 0.01$ ). Although there was no statistical significant difference in comet length for the primary myoblast comparison, the data appeared to follow a similar trend to that observed for the C2C12 myoblasts.

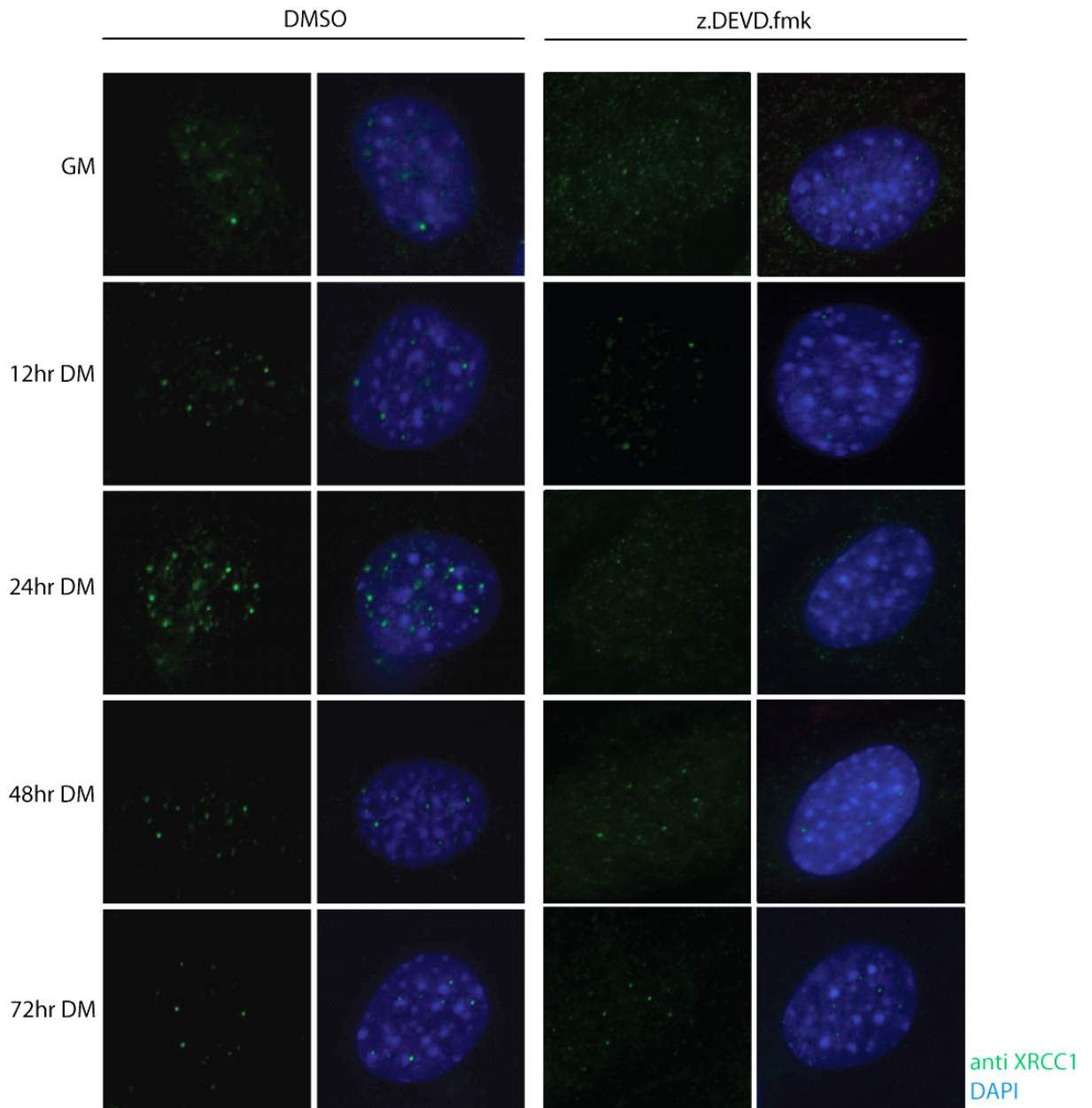


**Figure 11 Immunofluorescent staining for XRCC1 in caspase 3 inhibited differentiating C2C12 cells reveals a reduction in foci formation when caspase 3 is inhibited.**

Proliferating C2C12 cells were treated with a chemical inhibitor of caspase 3 (z.DEVD.fmk) (15 $\mu$ M) or with a DMSO vehicle only control 2hr prior to being induced to differentiate using low serum media also containing 15 $\mu$ M z.DEVD.fmk or DMSO. At the appropriate time points the cells were methanol fixed and immunofluorescently stained for XRCC1 with anti XRCC1 primary antibody (1:100) and Alexa498 secondary (1:500) and counter stained to show the nucleus using DAPI. Representative cells from n=3 experimental replicates are shown with the XRCC1 channel separate from the DAPI to show detailed staining patterns.

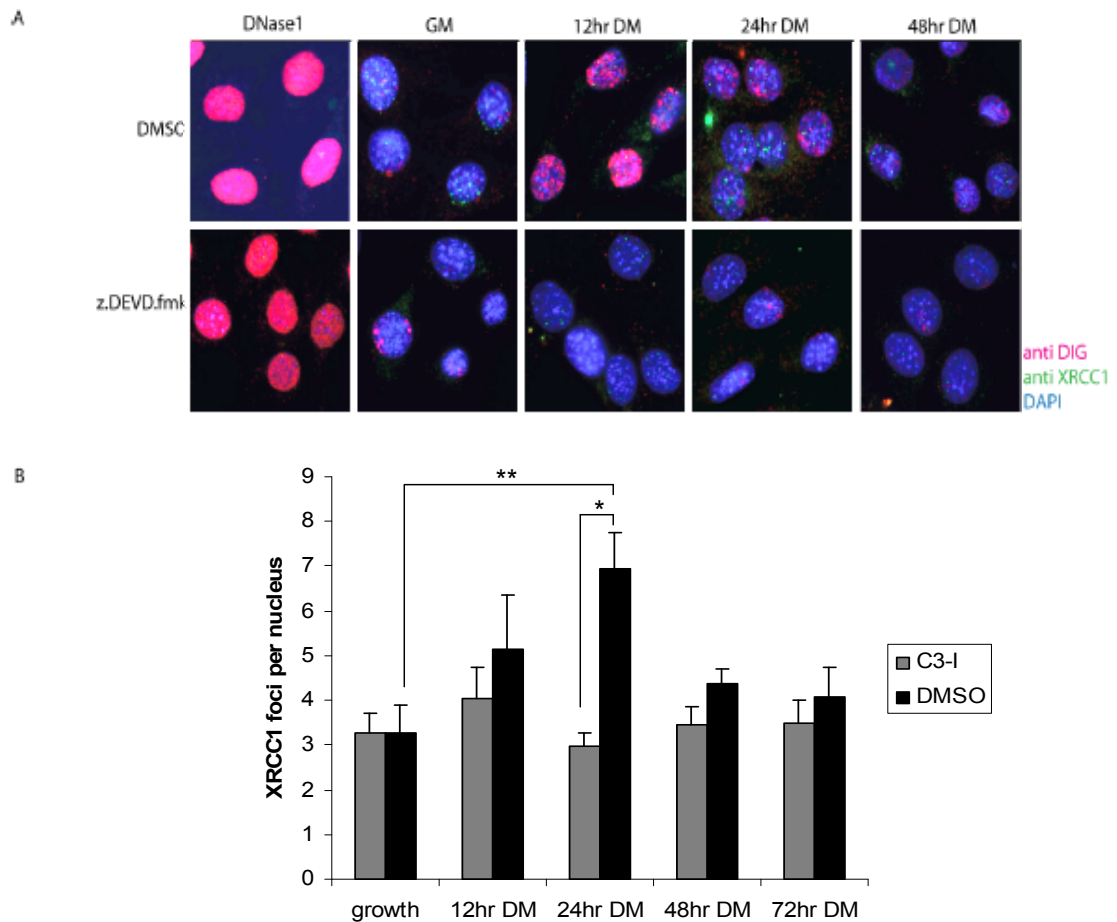


**Figure 12 DNA damage and XRCC1 foci formation is blocked by chemical inhibition of caspase 3 in differentiating C2C12 cells.**

Proliferating C2C12 cells were chemically inhibited for caspase 3 using 15 $\mu$ M z.DEVD.fmk in growth media 2hr prior to induction of differentiation. As a vehicle only control, control cells were treated 15 $\mu$ M DMSO. The cells were induced to differentiate using low serum media containing the same concentration of either z.DEVD.fmk or DMSO. A) At the appropriate time point the cells were methanol fixed and the ISNT assay was performed staining for DIGII and co staining for XRCC1. DAPI was used to counter stain the nucleus. B) The cells in five fields of view for n=3 experimental replicates were counted for appearance of nuclear XRCC1 foci in both the caspase 3 inhibited and vehicle only control conditions. The average from each experimental replicate was calculated and plotted. The y axis represents the average number of foci counted per condition. The stars (\*) indicate that the changes in foci formation between the two conditions indicated are statistically significant as determined by student t two tailed analysis with p<0.01

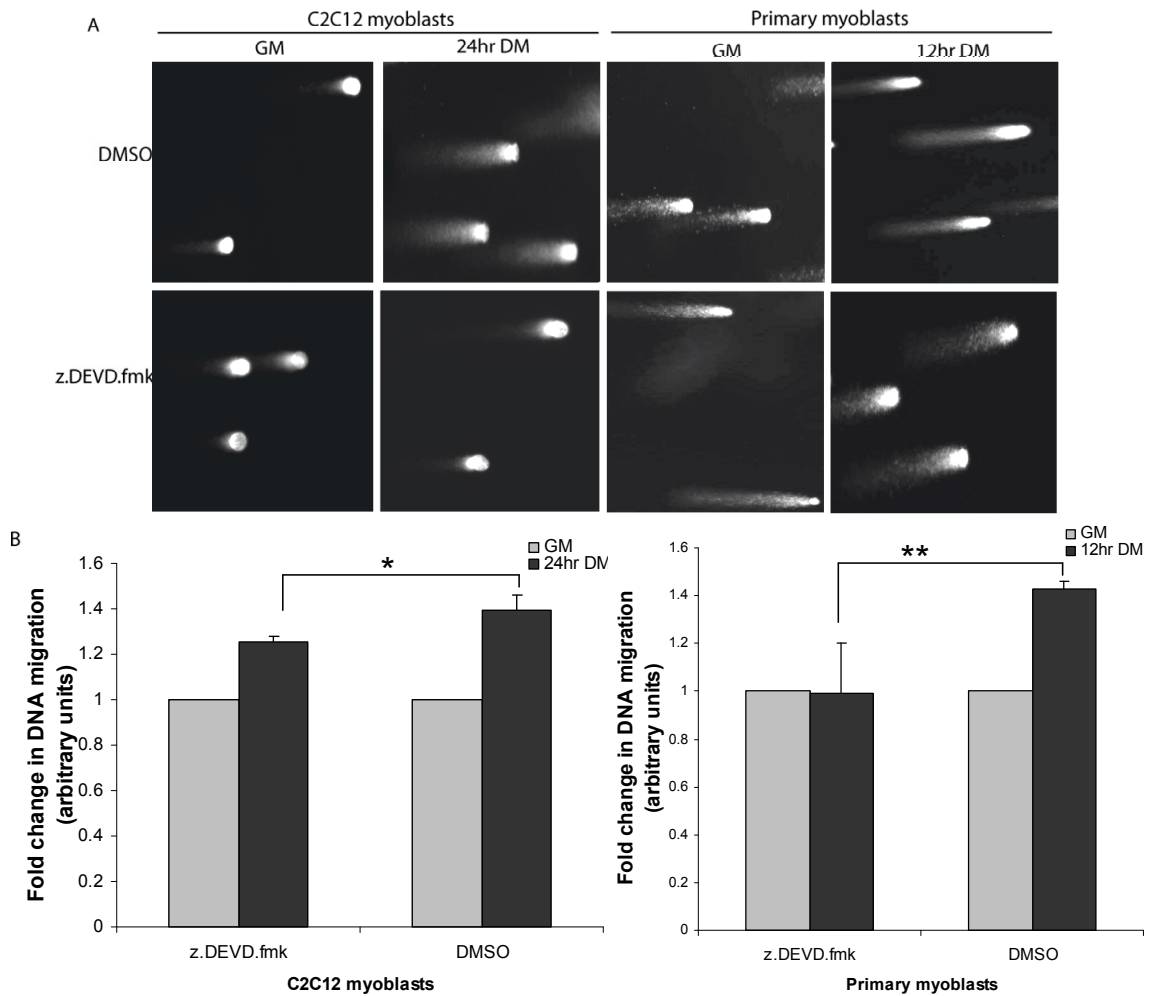


**Figure 13 DNA damage is reduced when caspase 3 is chemically inhibited in differentiating C2C12 myoblast cells as seen by a reduction in comet tail length.**

Proliferating primary myoblasts or C2C12 cells were chemically inhibited for caspase 3 or DMSO and induced to differentiate. The cells were collected intact and frozen at the appropriate time points. A) The comet assay was performed and representative images were taken at 20X magnification using a fluorescent microscope. B) The relative length of migration of concentrated DNA within each comet tail was measured for n=3 experimental replicates and normalized to the growth condition. The average fold change in migration length was plotted for each condition. The change in relative comet length was found to be statistically significant in both primary myoblast cells as well as in C2C12 myoblast cells using the student t two tail test with a p<0.05

### ***3.4 The effect of shRNA mediated knock down of XRCC1 gene expression in differentiating myoblasts.***

As noted above we have demonstrated that XRCC1 forms distinct nuclear foci in response to the induction of DNA lesions early in the differentiation program. Here we examined the impact of abrogating XRCC1 expression via shRNA mediated knock down on skeletal myoblast differentiation. shRNA or small hairpin RNA limits gene expression by targeting and binding to the mRNA sequence prior to the initiation of transcription. The shRNA targeted to the XRCC1 transcript did not contain a fluorescent label which limited the ability to successfully identify the cells that had been successfully transfected. To circumvent this limitation, co-transfection with a dsRED plasmid was performed. These plasmids were transfected at the same concentrations in the same transfection lysate (Lipofectamine 2000) to ensure that the micelles carried similar concentrations of each plasmid. Transfected myoblasts were then monitored by examining cell cultures under the rhodamine channel, following fixation in formaldehyde. This approach allowed for the quantification of successfully transfected myoblasts.

The transfected myoblasts were induced to differentiate and re-transfected following 48hrs to ensure that the XRCC1 targeted gene repression would be maintained through the duration of a differentiation time course. To assess the impact (if any) on differentiation, myoblasts were immunofluorescently stained for myosin heavy chain (MyHC). MyHC expression is up-regulated in newly formed myotubes/myofibers and its expression is a well established marker of terminal differentiation. In Figure 14

representative images of the immunofluorescent staining are presented. These images revealed that the successfully transfected myoblasts displayed a significant decrease in the expression of MyHC and in the formation of mature myotubes.

To assess the degree of XRCC1 KD in the cells qPCR was performed using the same primers designed to specifically amplify XRCC1 as were used in previous qPCR experiments. The qPCR results reveal that XRCC1 KD in the cells was approximately 50% in the growth condition (Figure 15 A). The transfection efficiency was calculated by counting the total number of dsRED positive cells and comparing that to the total number of cells. The transfection efficiency was determined to be approximately 30% in the case of both the XRCC1 shRNA and scrambled control shRNA conditions (Figure 15 B). Finally, the fusion index in both the XRCC1 and control KD conditions was monitored. To calculate the fusion index the total number of MyHC positive dsRED cells were compared to the total number of dsRED positive cells. This was calculated in both the XRCC1 and control KD conditions for all time points. When XRCC1 gene expression was limited in the shRNA treatment condition there was a dramatic reduction in the expression of MyHC positive myotubes to approximately 10% of the control shRNA treatment condition (Figure 15 C). These observations suggest that reductions in XRCC1 gene expression impair the ability of myoblasts to successfully complete the differentiation program.

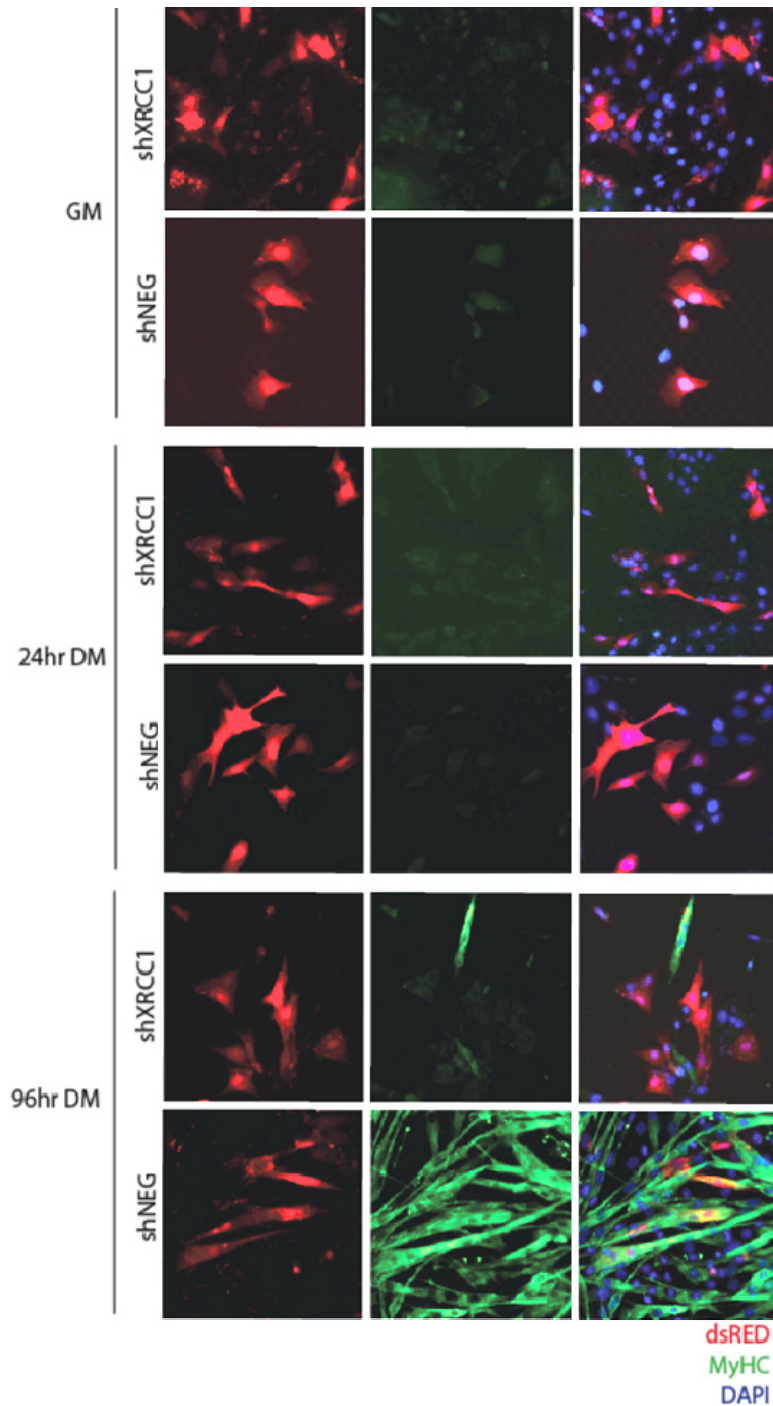


**Figure 14 shRNA mediated knock down of XRCC1 in differentiating C2C12 myoblast cells impairs the formation of myotubes.**

Proliferating C2C12 myoblast cells were co-transfected with dsRED plasmid and shRNA directed against XRCC1 or a scrambled shRNA negative control plasmid 24hr prior to being induced to differentiate using low serum media. The cells were fixed in 70% paraformaldehyde at the indicated time point. dsRED plasmid DNA was visualized using Cy3 channel of fluorescent microscope. The appearance of red staining indicates successful transfection of that cell. Immunofluorescent staining of myosin heavy chain using anti-MF20 antibody (1: 100) indicates that when XRCC1 is knocked down the cells are unable to form myotubes.

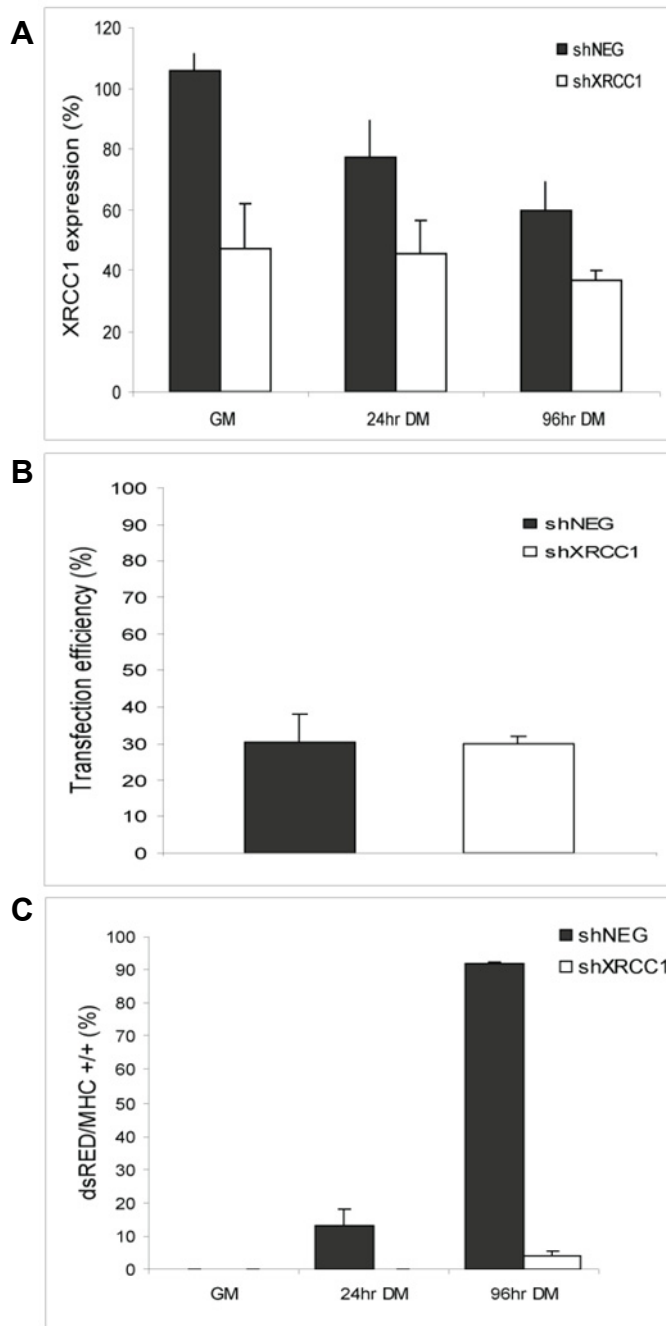


**Figure 15 Graphical analysis of shRNA mediated knock down of XRCC1 in differentiating C2C12 myoblasts.**

A) Differentiation index was calculated by counting dsRED positive MyHC positive cells versus all dsRED positive cells. B) Transfection efficiency was calculated by counting the number of dsRED positive cells versus total nuclei. C) Real time RT-PCR reveals that the shRNA transfection was able to reduce XRCC1 gene expression by 50% in proliferating cells.

## **4 Discussion**

#### ***4.1 The role of Caspase 3 and Caspase Activated Nuclease in the formation of DNA lesions during cellular differentiation.***

The results here clearly demonstrate that transient DNA lesions are induced during myoblast differentiation and that this process is immediately followed by focal accumulation of the DNA repair protein XRCC1. Prior observations have established that caspase 3 activity increases at time points that correspond to the induction of the observed DNA strand breaks and that caspase activity mediates the formation of these strand breaks through directed activation of the CAD nuclease. As such, the observations herein suggest that XRCC1 foci formation is a functional response to assist or direct DNA repair during myoblast differentiation.

Caspase 3 is emerging as a protease that is required not only for the successful induction of programmed cell death but also in cellular differentiation. Caspase 3 has been shown to be involved in the induction of differentiation of various cell types and in a diversity of species such as yeast, *Drosophila* and mouse (Fernando 2002). The mechanism by which caspase 3 activates the differentiation protocol is not well known but it is thought that it is acting through the cleavage of downstream substrates via aspartic acid cleavage sites. One such downstream target that has been shown to be activated by caspase 3 in both apoptosis and differentiation is a nuclease referred to as caspase activated DNase (CAD). During apoptosis CAD is responsible for cleaving DNA via its nuclease activity resulting in DNA fragments of 200bp lengths. The recent study of Larsen et al. (2010) has suggested that the differentiation associated activation of CAD may be limited when compared to CAD activation during apoptosis. This focal activation then is presumed to induce DNA damage but not complete nuclear

disruption. The damage induced by CAD in differentiating myoblasts is such that is easily manageable by an as of yet unknown repair mechanism. Indeed, in myoblasts that have a reduction in CAD expression there is a marked decrease in the ability of those same cells to undergo normal differentiation as well as a complete lack of DNA damage (Larsen, Rampalli et al. 2010).

Not only was the presence of CAD found to be required for myoblast differentiation, but a likely gene target was also described. Here, the authors reported that CAD specifically targeted the cyclin dependant kinase (CDK) inhibitor p21. The up-regulation of p21 is required in many cell types, including myoblasts, to facilitate exit from the cell cycle, a step critical for successful completion of cellular differentiation. Multiple DNA lesions were observed within the p21 promoter region upon induction of differentiation and the appearance of these lesions were dependent on endogenous caspase 3 activity (i.e. when caspase 3 was inhibited there was a block in the formation of detectable DNA damage in the p21 promoter). Of interest, no such lesions were detectable in the myogenin promoter region during differentiation. The collective interpretation of these observations suggested that the caspase 3/CAD directed DNA damage may act as an inductive signal for initiating gene expression associated with cell differentiation in general rather than a tissue or lineage specific gene expression program. In addition, the methylation status of the p21 promoter was not altered suggesting that the change in p21 gene expression observed did not originate from the removal of a repressive methylation environment (Larsen, Rampalli et al. 2010).

## ***4.2 Gene activation and the role of DNA repair proteins***

### **4.2.1 Single strand break repair proteins**

The current study demonstrates that DNA damage and its subsequent repair is required for the successful differentiation of myoblast cells. Nevertheless, the mechanism by which DNA damage and DNA repair alter gene expression remains unclear. An investigation of the literature reveals that the alteration of gene expression associated with other DNA damage and subsequent DNA repair events results from a modification of the immediate epigenetic environment, a change that may activate or repress gene expression from the affected loci.

Gene expression requires RNA polymerase II recruitment, transcription factors, co-activators and histone-modifying enzymes at the promoter. It has been reported that single strand break repair (SSBR) proteins have been implicated in the facilitation of chromatin modifications at active promoters in the absence of genotoxic stress. The alteration of chromatin produces changes in the epigenetic environment that are conducive to gene expression. Mutations in many SSBR genes have been associated with many human genetic disorders including; xeroderma pigmentosum, trichothiodystrophy, cockayne syndrome and cerebro-oculo-facio-skeletal syndrome. Interestingly it has been found that the majority of these syndromes are not associated with DNA repair deficiencies which leads to the argument that these proteins function in roles beyond those of DNA repair (Le May, Mota-Fernandes et al. 2010).

Many reports have indicated poly(ADP-ribose) polymerases (PARPs) in the involvement of chromatin remodeling and histone modification including transcription, DNA repair and differentiation. PARP has been strongly implicated in SSBR pathways and

is known to localize to sites of single strand breaks and recruit subsequent repair proteins such as XRCC1 via specific BRCA1 c-terminus (BRCT) binding domains as outlined in Figure S. 1. The recruitment of XRCC1 coordinates the further recruitment of ligase and polymerase proteins, DNA ligase III and DNA polymerase  $\beta$  respectively, which are responsible for processing the damaged DNA and religating the nick. The role of PARP may also moderate DNA damage and repair indirectly. For example, PARP is responsible for the poly(ADP-ribosyl)ation of histones which leads to decompaction of chromatin, thus allowing for the access of transcriptional machinery and the initiation of gene transcription. PARP also modifies the ability to exchange histone H1 for high mobility group proteins that, again, cause an opening up of chromatin thus facilitating transcription. Although there are many instances of PARP activation/inactivation causing a change in the histone code and a corresponding change in gene regulation still the physiological activators of PARP remains elusive. However, one well known activation signal for PARP is that which occurs upon the detection of DNA damage. In addition, PARP is able to alter the histone code by adding poly(ADP-ribose) in chains to the histones that are targeted alleviating the compaction of the nucleosome. Therefore, it is reasonable to assume that PARP may alter gene expression in regions of DNA damage through one or multiple mechanisms (Quenet, El Ramy et al. 2009). Such a method of gene activation would be very rapid and, in the context of CAD activated DNA damage seen in differentiation, would be genome wide causing a rapid change in gene regulation at the level of the histone code. Interestingly, the PAR chains are also required for recruiting not only repair factors but it may also be implicated in the

recruitment of histone modification factors as well as DNA methyltransferases, which further promote gene transcription (Quenet, Gasser et al. 2008).

#### **4.2.2 Double strand break repair proteins**

The DNA damage response (DDR) in vertebrate cells describes the coordination of DNA repair proteins that become activated upon genetic insult whether by extrinsic factors such as ionizing radiation or intrinsic factors such as reactive oxygen species or stalled replication forks. As described in Section 1.4 there are multiple pathways and proteins that become activated in order to minimize the damaging effects of DNA lesions within the cell. Without a DDR the cell is at risk of apoptosis, genome instability and mutation, and perhaps even causing harm to the host organism by propagating deleterious mutations within the progeny (Harrison and Haber 2006). One of the main players in the DDR, specifically in the response to dsDNA damage, is ataxia telangiectasia mutated (ATM). The role of ATM is to detect DNA damage and phosphorylate other key proteins causing their activation. For example ATM causes the phosphorylation of histone H2AX upon recognition of DNA damage and this phosphorylation leads to the recruitment of other repair factors to the site of damage. Another target of ATM is the phosphorylation of the tumour suppressor protein p53 in response to DNA damage. This phosphorylation activates the protein which leads to growth arrest in the cell (Banin, Moyal et al. 1998). The activation of ATM was not detected at a 12hr post low serum induced differentiation in myoblasts but there was a detection of  $\gamma$ H2AX as described in Figure S2. This may indicate that the activation of ATM occurs very early in differentiation or not at all. The role of p53 can be to induce

DNA repair or, in cases where the genetic damage is too severe, it can induce apoptosis and it may be activated by many cues. One of the targets of p53 is the upregulation of the cyclin dependent kinase inhibitor p21 (Kim 1997). When p21 is upregulated this causes the cell to exit the cell cycle at G1 so that it can no longer undergo replication. In recent work out of the Megeney lab it has been demonstrated by ligation mediated PCR that there are consistent DNA breaks that are observed in the promoter region of p21 at early time points in differentiating myoblast cells. These breaks were no longer detected in terminally differentiated cells (Larsen, Rampalli et al. 2010). It is conceivable that the damage observed is not only targeting specific genes for up/down regulation by altering the chromatin environment but it also may be that the global DNA damage observed may be responsible for the activation of DNA repair machinery that is also able to contribute to eliciting differentiation cues. An example of this may be the recruitment of PARP to sites of DNA damage in order to relax chromatin condensation. The observed recruitment of PARP to TopoII $\beta$  induced DNA lesions in glucocorticoid sensitive genes leads to upregulation of those genes by causing poly(ADP ribose)ylation and ultimately an exchange of histone H1 for HMGB which allows for access of DNA transcription machinery to the promoter region of those genes. The damage observed in differentiation may be responsible for causing the recruitment of PARP and similar repair factors that may be able contribute to an increase in transcription of the genes required for differentiation (Ju, Lunyak et al. 2006). The activation of p53 has been observed in the differentiation program of stem cells and progenitor cells such as hematopoietic stem cells and glioma cells respectively. In these cell types the activation

of p53 is crucial for differentiation to occur. Without the activation of p53 the cells maintain a proliferative state and will not exit the cell cycle to terminally differentiate (Liu, Elf et al. 2009). It has also been reported that dedifferentiation of induced pluripotent stem cells is aided by an inhibition of p53 (Kawamura, Suzuki et al. 2009). Although p53 is able to induce apoptosis when the cell is under extreme stress it is likely that if there is p53 activation involved in skeletal muscle differentiation is not via this mechanism. Since differentiating cells are not undergoing apoptosis even though there is activation of key players of the apoptotic cascade observed in differentiating cells such as caspase 3 and CAD it is feasible that the activation signal is one that does not require p53. The activation of the caspase cascade in differentiating cells occurs in a dosage dependant manner in that the increase in caspase 3 activity observed in differentiating myoblasts is only a fraction of what is observed in cells undergoing apoptosis and it is detected transiently in early time points of differentiation only (Fernando, Kelly et al. 2002). It is therefore conceivable that the activation of the caspase cascade and the potential activation of p53 may occur through differing mechanism but occur ultimately in the same differentiation program.

#### ***4.3 XRCC1 and its possible contribution to DNA damage repair in skeletal muscle differentiation.***

The role of X-ray repair cross-complimenting protein 1 (XRCC1) in DNA repair is to coordinate the multitude of enzymatic components that are required to detect, process and religate DNA lesions. XRCC1 has been implicated in single strand break repair as it acts through the base excision repair pathway and in double strand break repair as it

acts through the backup or PARP-1 dependant non-homologous end joining pathway. XRCC1 itself has no enzymatic activity; rather it acts as a scaffold protein to bind and coalesce various repair proteins through multiple binding domains. For example, XRCC1 is known to physically interact with PARP-1, APE1, DNA polymerase  $\beta$ , DNA PK and DNA ligase III. When a DNA lesion is detected PARP-1 is recruited to the site of damage through its DNA binding domain. XRCC1 subsequently binds PARP-1 via its centrally located BRCT domain. This domain is found in many proteins involved in the DNA damage response and cell cycle check points (Masson, Niedergang et al. 1998). Once XRCC1 is bound at the site of the lesion it coordinates the binding of additional proteins that are recruited to the site by the poly(ADP-ribosyl)ation activity of PARP (El-Khamisy, Masutani et al. 2003). DNA ligase III is bound to XRCC1 by a second C-terminal BRCT domain while DNA pol $\beta$  is bound to the N-terminal end. For successful processing and closing of the DNA lesion, the proteins need to be in close proximity and XRCC1 provides the means for these proteins to be coordinated in physical space (Masson, Niedergang et al. 1998).

SSBR deficiencies have been linked to the development of a variety of neurodegenerative diseases such as spinocerebellar ataxia with axonal neuropathy (SCAN1) and ataxia with oculomotor apaxia (AOA1). However, XRCC1 has also been linked, albeit indirectly, to the control of cell differentiation in the brain. Here, investigators examined the effect of conditional loss of XRCC1 in the nervous system of mice. Generation of XRCC1 null mice is embryonic lethal (usually around day 7), as such an engineered XRCC1 loxP conditional knock out model was generated using a Nestin

driven CRE to abolish XRCC1 in all cells of the nervous system (Lee, Katyal et al. 2009). Neuronal loss of XRCC1 resulted in delayed growth, a 25% decrease in whole brain size and the adult onset of neurological dysfunction marked by ataxia and spasms. Closer inspection of the brains of the XRCC1<sup>Nes-cre</sup> mice revealed that the cerebellum in particular exhibited a widespread loss in mass compared to the other areas of the brain. Interestingly, there was a decrease in the ability of the cerebellar interneurons to differentiate when XRCC1 was abolished, although the differentiation deficit was not observed in any other cell types of the cerebellum. Development of the cerebellar interneurons occurs postnatally from migrating progenitor cells that are located in the white matter of the cerebellum suggesting that this form of post-natal neuronal differentiation is sensitive to or dependent on a functional XRCC1 protein. In addition to the cerebellar defect, XRCC1<sup>Nes-cre</sup> animals also displayed abnormal hippocampal activity leading to the generation of seizures in the adult mice. Although there was no clear rationale to explain this phenotype, such an abnormal function may originate from a defect in the differentiation process in this region of the brain. For example, while the hippocampus may have retained an outward morphology consistent with normal function, a subtle alteration in maturation/differentiation may have lead to the increased susceptibility to altered activity. Nevertheless, the evidence of this study strongly suggests that XRCC1 is essential for the genesis of cerebellar interneurons and normal hippocampal function ((Lee, Katyal et al. 2009).

#### ***4.4 Future experimental directions to elucidate candidate repair pathways/proteins that moderate cell differentiation***

The experiments outlined here have begun to unravel the ambiguity of which DNA repair mechanism may be involved in the response to DNA damage during myoblast differentiation. Many key experiments remain to be performed in order to make a precise claim as to the exact mechanism that mediates this process. The role of PARP in differentiation associated DNA damage and repair remains undefined. As PARP is down regulated in apoptosis through caspase directed cleavage, it may be reasonable to assume that a similar process occurs during differentiation. However, PARP cleavage has not been observed over a differentiation time course in myoblasts (Fernando et al. 2002). Therefore, a pool of PARP may remain intact or there may be a surge in PARP expression to ensure that this protein can localize to the sites of DNA damage in differentiating cells. The expression of PARP appears to remain fairly consistent through growth and into the early time points of differentiation (Figure 7), suggesting that a continual replenishment of PARP is occurring. To clarify the role of PARP in this process a number of experiments could be performed including immunofluorescent staining for PARP, examination of the co-localization of PARP and XRCC1, as well as gene disruption of PARP during myoblast differentiation.

As a means to place XRCC1 at a site of DNA damage during myoblast differentiation, chromatin immunoprecipitation (ChIP) experiments could be performed at the p21 promoter region. A ChIP experiment crosslinks any proteins to their site of DNA binding *in vitro* by formaldehyde crosslink formation. The protein of interest is then immobilized on specifically labeled beads then the cross links are removed and any

bound DNA is collected and amplified for the region of interest. In this case XRCC1 would be immobilized to the beads via antibody interaction and the resulting DNA would be amplified using p21 promoter specific primers. Evidence of enrichment of XRCC1 at the p21 promoter (at the same sites identified as CAD directed DNA damage locations) would be a significant observation and would provide compelling evidence implicating an XRCC1 repair pathway in myoblast differentiation. Similar experiments could also be conducted looking at locations of PARP association at the p21 promoter region.

In addition to these *in vitro* based experiments, *in vivo* analysis should also be conducted to confirm a role for XRCC1 in the ambient DNA repair process during myoblast differentiation. The existing XRCC1 knock out (KO) model is embryonic lethal which precludes use of this resource to address skeletal muscle differentiation. However, to circumvent this limitation, use of a conditional KO model can be contemplated. Here, one could envisage use of the XRCC1 floxed mouse (as described by Lee, Katyal et al. 2009) crossed with a Myf5 Cre mouse to generate a skeletal muscle specific XRCC1 deletion. These mice could then be utilized to address the *in vivo* role of XRCC1, whether loss of XRCC1 leads to alterations in skeletal muscle development; whether primary myoblasts derived from these mice display abnormalities in differentiation etc. we would be able to observe the effects of the loss XRCC1 in developing muscle tissue.

#### ***4.5 Final Summary and Conclusion***

Early Caspase 3 activation is required in the differentiation program of myoblasts to activate downstream targets such as the caspase activated nuclease (CAD). The activation of CAD was found to induce genome wide DNA lesions early in differentiation. The lesions observed were found to be absent in the late time points of differentiation and were not present in proliferating cells. Here, using the alkaline comet assay, we found corroborating evidence that DNA lesions are induced in differentiating cells. Also observed, by means of ISNT, was that the formation of DNA lesions were abrogated in cells where caspase 3 was chemically inhibited. The formation and subsequent absence of DNA damage in the differentiation time course suggested that an active DNA repair process was engaged to repair the insult caused by CAD activity.

To explore the possible mechanism involved in DNA repair, gene and protein expression levels of many candidate repair proteins were examined. Protein localization analysis by immunofluorescent staining revealed that XRCC1 exhibited a significant change in localization during and immediately following the peak elevation in DNA damage. XRCC1 is a scaffold protein typically implicated in single strand break repair and to a lesser extent in the backup non-homologous end joining double strand break repair pathway. The role of XRCC1 in these pathways is to coordinate the binding of the multitude of repair proteins recruited upon detection of DNA damage.

Further evidence of the involvement of XRCC1 in differentiation came from the observation that the localization of XRCC1 into punctate foci was dramatically reduced when myoblasts were exposed to chemical inhibitors of caspase 3. Additionally, XRCC1

expression level was knocked down in C2C12 myoblast cells via shRNA and the ability of the cells to differentiate was observed. In these cells it was found that, when the XRCC1 shRNA was successfully transfected, there was a decrease in the ability of those cells to differentiate as seen by a lack of myosin heavy chain expression. MyHC is upregulated in myotubes and an increase in expression is a marker of late stage skeletal muscle differentiation.

Further experimentation is required to show with greater impact that XRCC1 is in fact one of the proteins required for the repair of DNA damage induced in differentiation. As well as XRCC1 other likely candidates should also be examined further such as PARP-1 which is known to bind XRCC1 after binding to DNA at the site of damage. It has previously been observed in neural tissue specific knockout mice that a loss of XRCC1 expression is deleterious to the development of cerebellar interneurons and hippocampal function. Study of a skeletal muscle specific XRCC1 knock out *in vivo* should provide some insight into the effects of DNA repair defects on the ability of muscle to develop and/or regenerate in an animal model.

The experimental results indicate that the repair mechanism responsible for repairing the caspase 3/CAD induced DNA damage observed in the differentiation of skeletal muscle likely involves XRCC1 as a means to coordinate the repair. It remains unclear whether the break repair mechanism employed is one that repairs single strand breaks such as base excision repair or one that repairs double strand breaks such as B-NHEJ. Future experiments should be performed to explore which of the candidate mechanism is implicated in the repair observed in skeletal muscle differentiation.

## **5 References**

- Abdul-Ghani, M., D. Dufort, et al. (2011). "Wnt11 promotes cardiomyocyte development by caspase-mediated suppression of canonical Wnt signals." Mol Cell Biol **31**(1): 163-78.
- Adrain, C. and S. J. Martin (2001). "The mitochondrial apoptosome: a killer unleashed by the cytochrome seas." Trends Biochem Sci **26**(6): 390-7.
- Almeida, K. H. and R. W. Sobol (2007). "A unified view of base excision repair: lesion-dependent protein complexes regulated by post-translational modification." DNA Repair (Amst) **6**(6): 695-711.
- Audebert, M., B. Salles, et al. (2004). "Involvement of poly(ADP-ribose) polymerase-1 and XRCC1/DNA ligase III in an alternative route for DNA double-strand breaks rejoining." J Biol Chem **279**(53): 55117-26.
- Audebert, M., B. Salles, et al. (2008). "Effect of double-strand break DNA sequence on the PARP-1 NHEJ pathway." Biochem Biophys Res Commun **369**(3): 982-8.
- Banin, S., L. Moyal, et al. (1998). "Enhanced phosphorylation of p53 by ATM in response to DNA damage." Science **281**(5383): 1674-7.
- Bergstrom, D. A. and S. J. Tapscott (2001). "Molecular distinction between specification and differentiation in the myogenic basic helix-loop-helix transcription factor family." Mol Cell Biol **21**(7): 2404-12.
- Buckingham, M., L. Bajard, et al. (2003). "The formation of skeletal muscle: from somite to limb." J Anat **202**(1): 59-68.
- Burma, S., B. P. Chen, et al. (2006). "Role of non-homologous end joining (NHEJ) in maintaining genomic integrity." DNA Repair (Amst) **5**(9-10): 1042-8.
- Carvalho, A. B. (2003). "The advantages of recombination." Nat Genet **34**(2): 128-9.
- Chao, D. T. and S. J. Korsmeyer (1998). "BCL-2 family: regulators of cell death." Annu Rev Immunol **16**: 395-419.
- Chinnaiyan, A. M., K. O'Rourke, et al. (1995). "FADD, a novel death domain-containing protein, interacts with the death domain of Fas and initiates apoptosis." Cell **81**(4): 505-12.
- Cornelison, D. D. and B. J. Wold (1997). "Single-cell analysis of regulatory gene expression in quiescent and activated mouse skeletal muscle satellite cells." Dev Biol **191**(2): 270-83.
- Deans, B., C. S. Griffin, et al. (2003). "Homologous recombination deficiency leads to profound genetic instability in cells derived from Xrcc2-knockout mice." Cancer Res **63**(23): 8181-7.
- Dianov, G. L. and J. L. Parsons (2007). "Co-ordination of DNA single strand break repair." DNA Repair (Amst) **6**(4): 454-60.
- El-Khamisy, S. F., M. Masutani, et al. (2003). "A requirement for PARP-1 for the assembly or stability of XRCC1 nuclear foci at sites of oxidative DNA damage." Nucleic Acids Res **31**(19): 5526-33.
- Enari, M., H. Sakahira, et al. (1998). "A caspase-activated DNase that degrades DNA during apoptosis, and its inhibitor ICAD." Nature **391**(6662): 43-50.
- Fernando, P. (2002). "Caspase 3 activity is required for skeletal muscle differentiation." Proceedings of the National Academy of Sciences **99**(17): 11025-11030.

- Fernando, P., S. Brunette, et al. (2005). "Neural stem cell differentiation is dependent upon endogenous caspase 3 activity." *FASEB J* **19**(12): 1671-3.
- Fernando, P., J. F. Kelly, et al. (2002). "Caspase 3 activity is required for skeletal muscle differentiation." *Proc Natl Acad Sci U S A* **99**(17): 11025-30.
- Fernando, P. and L. A. Megeney (2007). "Is caspase-dependent apoptosis only cell differentiation taken to the extreme?" *FASEB J* **21**(1): 8-17.
- Finucane, D. M., E. Bossy-Wetzel, et al. (1999). "Bax-induced caspase activation and apoptosis via cytochrome c release from mitochondria is inhibitable by Bcl-xL." *J Biol Chem* **274**(4): 2225-33.
- Frank, K. M., J. M. Sekiguchi, et al. (1998). "Late embryonic lethality and impaired V(D)J recombination in mice lacking DNA ligase IV." *Nature* **396**(6707): 173-7.
- Freer-Prokop, M., J. O'Flaherty, et al. (2009). "Non-canonical role for the TRAIL receptor DR5/FADD/caspase pathway in the regulation of MyoD expression and skeletal myoblast differentiation." *Differentiation* **78**(4): 205-12.
- Fujita, J., A. Crane, et al. (2008). "Caspase Activity Mediates the Differentiation of Embryonic Stem Cells." *Cell Stem Cell* **2**(6): 595-601.
- Gayraud-Morel, B., F. Chretien, et al. (2007). "A role for the myogenic determination gene Myf5 in adult regenerative myogenesis." *Dev Biol* **312**(1): 13-28.
- Gellert, M. (2002). "V(D)J recombination: RAG proteins, repair factors, and regulation." *Annu Rev Biochem* **71**: 101-32.
- Graves, J. D., Y. Gotoh, et al. (1998). "Caspase-mediated activation and induction of apoptosis by the mammalian Ste20-like kinase Mst1." *Embo J* **17**(8): 2224-34.
- Haince, J. F., M. Rouleau, et al. (2006). "Transcription. Gene expression needs a break to unwind before carrying on." *Science* **312**(5781): 1752-3.
- Harrison, J. C. and J. E. Haber (2006). "Surviving the breakup: the DNA damage checkpoint." *Annu Rev Genet* **40**: 209-35.
- Haupt, S., M. Berger, et al. (2003). "Apoptosis - the p53 network." *J Cell Sci* **116**(Pt 20): 4077-85.
- Hill, M., A. Wernig, et al. (2003). "Muscle satellite (stem) cell activation during local tissue injury and repair." *J Anat* **203**(1): 89-99.
- Hossain, M. S., N. Akimitsu, et al. (2003). "Myogenic differentiation of Drosophila Schneider cells by DNA double-strand break-inducing drugs." *Differentiation* **71**(4-5): 271-80.
- Iliakis, G., H. Wang, et al. (2004). "Mechanisms of DNA double strand break repair and chromosome aberration formation." *Cytogenet Genome Res* **104**(1-4): 14-20.
- Inomata, K., T. Aoto, et al. (2009). "Genotoxic Stress Abrogates Renewal of Melanocyte Stem Cells by Triggering Their Differentiation." *Cell* **137**(6): 1088-1099.
- Ishizaki, Y., M. D. Jacobson, et al. (1998). "A role for caspases in lens fiber differentiation." *J Cell Biol* **140**(1): 153-8.
- Ju, B. G., V. V. Lunyak, et al. (2006). "A topoisomerase IIbeta-mediated dsDNA break required for regulated transcription." *Science* **312**(5781): 1798-802.
- Kawamura, T., J. Suzuki, et al. (2009). "Linking the p53 tumour suppressor pathway to somatic cell reprogramming." *Nature* **460**(7259): 1140-4.

- Keren, A., Y. Tamir, et al. (2006). "The p38 MAPK signaling pathway: A major regulator of skeletal muscle development." Molecular and Cellular Endocrinology **252**(1-2): 224-230.
- Kim, T. K. (1997). "In vitro transcriptional activation of p21 promoter by p53." Biochem Biophys Res Commun **234**(2): 300-2.
- Kuang, S., S. B. Charge, et al. (2006). "Distinct roles for Pax7 and Pax3 in adult regenerative myogenesis." J Cell Biol **172**(1): 103-13.
- Larsen, B. D., S. Rampalli, et al. (2010). "Caspase 3/caspase-activated DNase promote cell differentiation by inducing DNA strand breaks." Proc Natl Acad Sci U S A **107**(9): 4230-5.
- Larsen, B. D., S. Rampalli, et al. (2010). "Caspase 3/caspase-activated DNase promote cell differentiation by inducing DNA strand breaks." Proceedings of the National Academy of Sciences **107**(9): 4230-4235.
- Le Grand, F. and M. A. Rudnicki (2007). "Skeletal muscle satellite cells and adult myogenesis." Curr Opin Cell Biol **19**(6): 628-33.
- Le May, N., D. Mota-Fernandes, et al. (2010). "NER factors are recruited to active promoters and facilitate chromatin modification for transcription in the absence of exogenous genotoxic attack." Mol Cell **38**(1): 54-66.
- Lee, Y., S. Katyal, et al. (2009). "The genesis of cerebellar interneurons and the prevention of neural DNA damage require XRCC1." Nat Neurosci **12**(8): 973-80.
- Li, J. and J. Yuan (2008). "Caspases in apoptosis and beyond." Oncogene **27**(48): 6194-6206.
- Lieber, M. R., Y. Ma, et al. (2003). "Mechanism and regulation of human non-homologous DNA end-joining." Nat Rev Mol Cell Biol **4**(9): 712-20.
- Liu, Y., S. E. Elf, et al. (2009). "p53 regulates hematopoietic stem cell quiescence." Cell Stem Cell **4**(1): 37-48.
- Lyu, Y. L., C. P. Lin, et al. (2006). "Role of topoisomerase IIbeta in the expression of developmentally regulated genes." Mol Cell Biol **26**(21): 7929-41.
- Masson, M., C. Niedergang, et al. (1998). "XRCC1 is specifically associated with poly(ADP-ribose) polymerase and negatively regulates its activity following DNA damage." Mol Cell Biol **18**(6): 3563-71.
- Munsterberg, A. E., J. Kitajewski, et al. (1995). "Combinatorial signaling by Sonic hedgehog and Wnt family members induces myogenic bHLH gene expression in the somite." Genes Dev **9**(23): 2911-22.
- Murray, T. V., J. M. McMahon, et al. (2008). "A non-apoptotic role for caspase-9 in muscle differentiation." J Cell Sci **121**(Pt 22): 3786-93.
- Olguin, H. C. and B. B. Olwin (2004). "Pax-7 up-regulation inhibits myogenesis and cell cycle progression in satellite cells: a potential mechanism for self-renewal." Dev Biol **275**(2): 375-88.
- Oliver, F. J., G. de la Rubia, et al. (1998). "Importance of poly(ADP-ribose) polymerase and its cleavage in apoptosis. Lesson from an uncleavable mutant." J Biol Chem **273**(50): 33533-9.
- Otto, A., H. Collins-Hooper, et al. (2009). "The origin, molecular regulation and therapeutic potential of myogenic stem cell populations." J Anat **215**(5): 477-97.

- Penn, B. H., D. A. Bergstrom, et al. (2004). "A MyoD-generated feed-forward circuit temporally patterns gene expression during skeletal muscle differentiation." Genes Dev **18**(19): 2348-53.
- Quenet, D., R. El Ramy, et al. (2009). "The role of poly(ADP-ribosyl)ation in epigenetic events." Int J Biochem Cell Biol **41**(1): 60-5.
- Quenet, D., V. Gasser, et al. (2008). "The histone subcode: poly(ADP-ribose) polymerase-1 (Parp-1) and Parp-2 control cell differentiation by regulating the transcriptional intermediary factor TIF1beta and the heterochromatin protein HP1alpha." FASEB J **22**(11): 3853-65.
- Rivera-Munoz, P., L. Malivert, et al. (2007). "DNA repair and the immune system: From V(D)J recombination to aging lymphocytes." Eur J Immunol **37** Suppl 1: S71-82.
- Robertson, J. D., S. Orrenius, et al. (2000). "Review: nuclear events in apoptosis." J Struct Biol **129**(2-3): 346-58.
- Rosidi, B., M. Wang, et al. (2008). "Histone H1 functions as a stimulatory factor in backup pathways of NHEJ." Nucleic Acids Res **36**(5): 1610-23.
- Sabourin, L. A., A. Girgis-Gabardo, et al. (1999). "Reduced differentiation potential of primary MyoD<sup>-/-</sup> myogenic cells derived from adult skeletal muscle." J Cell Biol **144**(4): 631-43.
- Sakahira, H., M. Enari, et al. (1999). "Apoptotic nuclear morphological change without DNA fragmentation." Curr Biol **9**(10): 543-6.
- Seale, P., L. A. Sabourin, et al. (2000). "Pax7 is required for the specification of myogenic satellite cells." Cell **102**(6): 777-86.
- Szymczyk, K. H., T. A. Freeman, et al. (2006). "Active caspase-3 is required for osteoclast differentiation." J Cell Physiol **209**(3): 836-44.
- Tatsumi, R., A. Hattori, et al. (2002). "Release of hepatocyte growth factor from mechanically stretched skeletal muscle satellite cells and role of pH and nitric oxide." Mol Biol Cell **13**(8): 2909-18.
- Taylor, R. C., S. P. Cullen, et al. (2008). "Apoptosis: controlled demolition at the cellular level." Nat Rev Mol Cell Biol **9**(3): 231-41.
- Weterings, E. and D. J. Chen (2008). "The endless tale of non-homologous end-joining." Cell Research **18**(1): 114-124.
- Whitby, M. C. (2005). "Making crossovers during meiosis." Biochem Soc Trans **33**(Pt 6): 1451-5.
- Wu, Z., P. J. Woodring, et al. (2000). "p38 and extracellular signal-regulated kinases regulate the myogenic program at multiple steps." Mol Cell Biol **20**(11): 3951-64.
- Yi, X., X. M. Yin, et al. (2003). "Inhibition of Bid-induced apoptosis by Bcl-2. tBid insertion, Bax translocation, and Bax/Bak oligomerization suppressed." J Biol Chem **278**(19): 16992-9.
- Zermati, Y., C. Garrido, et al. (2001). "Caspase activation is required for terminal erythroid differentiation." J Exp Med **193**(2): 247-54.
- Zhang, P., C. Wong, et al. (1999). "p21(CIP1) and p57(KIP2) control muscle differentiation at the myogenin step." Genes Dev **13**(2): 213-24.
- Ziel, K. A., V. Grishko, et al. (2005). "Oxidants in signal transduction: impact on DNA integrity and gene expression." Faseb J **19**(3): 387-94.

## **6 Appendix**

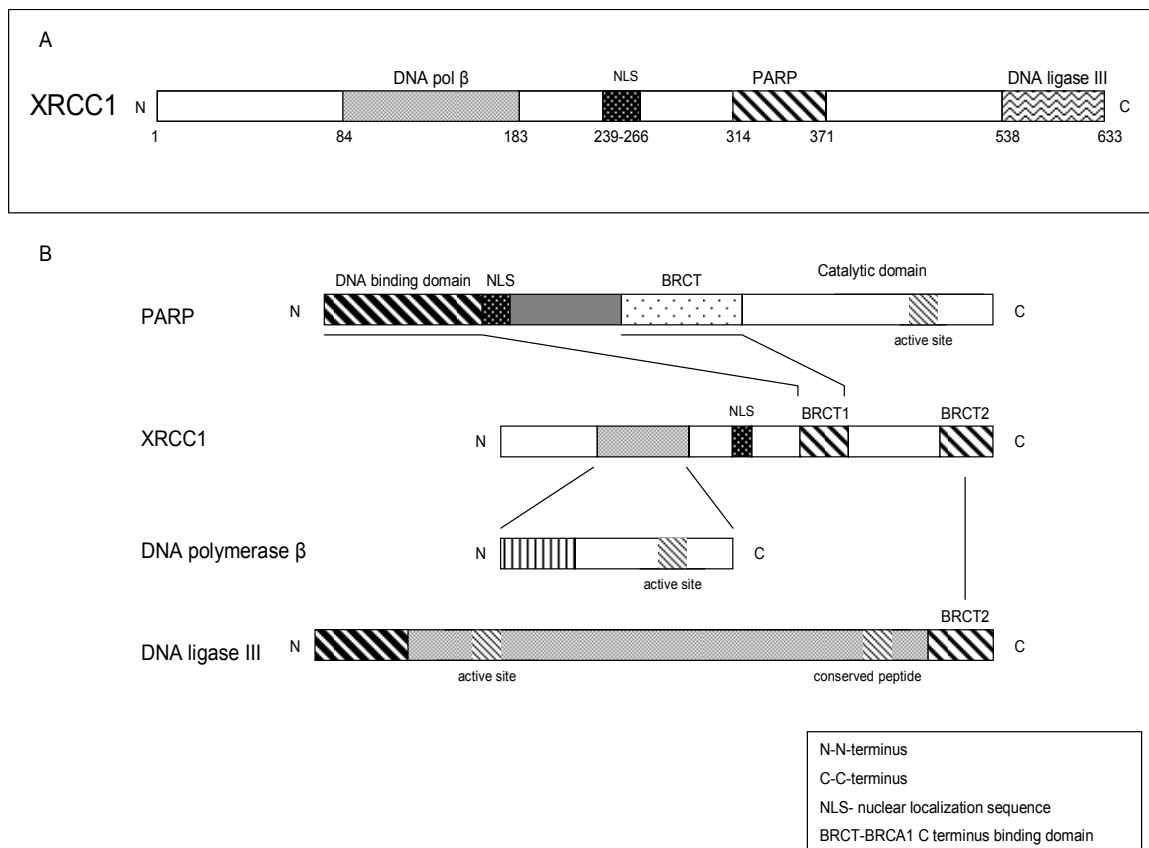


**Figure S. 1 Peptide map of XRCC1 and its binding partners in single strand break repair**

A) The location DNA repair protein binding domains on the XRCC1 peptide. Amino acids 1-84 of the XRCC1 peptide comprise the N terminal domain, 85-183 comprise the DNA polymerase  $\beta$  binding domain, 239-266 comprise the nuclear localization sequence, 314-371 comprise the PARP binding domain, and the C terminal region of amino acids 538-633 make up the DNA ligase III binding domain. B) The location and order of binding of single strand break repair proteins in response to DNA damage.

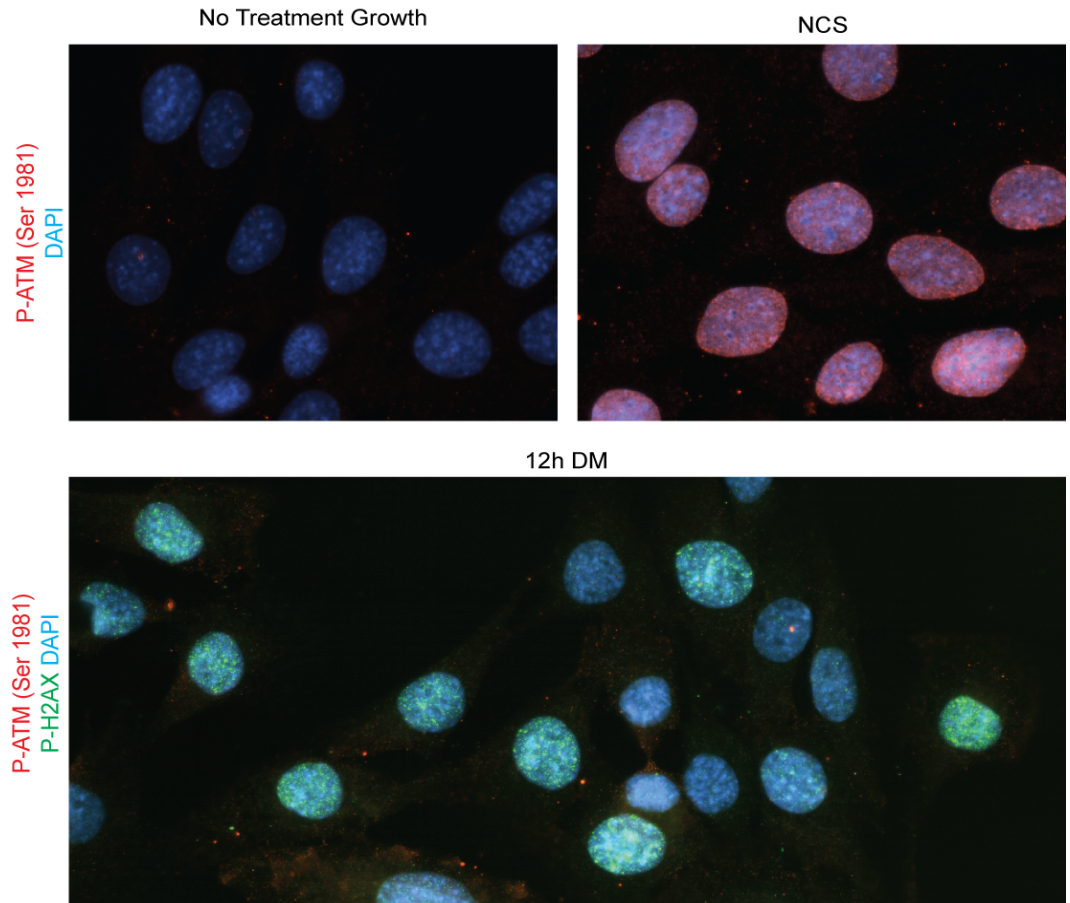


**Figure S. 2 Change in ATM expression and/or localization was not observed early in skeletal muscle differentiation.**

Proliferating C2C12 myoblast were treated with or without neocarzinostatin (NCS), fixed, and ATM activity was assessed by staining for ATM phosphorylation at serine 1981 (red). Nuclei were counter stained with DAPI. Differentiating C2C12 myoblasts were fixed 12 hours after the induction of differentiation and stained for P-H2AX (green), P-ATM (S1981) (red), and nuclei counterstained with DAPI (blue). P-ATM(S1981) did not correspond to the P-H2AX foci.

**Table 1 DNA primers used for RT PRC amplification of cDNA in differentiating C2C12 myoblasts**

<b>PARP-1 left</b> 5'- TGAGAAACTCGGAGGCAAGT- 3'	<b>PARP-1 right</b> 5'- CACCCTTGCTCTTCTTGGAG -3'
<b>DNA-PKcs left</b> 5'- GAGGCCATGATGAAAAGGAA-3'	<b>DNA-PKcs right</b> 5'- CGCTTTGGGGTCACTGTTAT-3'
<b>Artemis left</b> 5'- TGGCTCACAACCATCCATAA -3'	<b>Artemis right</b> 5'- GAAGGTGCCTGCTCCTACTG -3'
<b>Rad51 left</b> 5'- GCTCCTTTACCAAGCGTCAG -3'	<b>Rad51 right</b> 5'- GTTCCCTCCAATGGGTTTTTT-3'
<b>APE1 left</b> 5'- CAGTGCCCGCTAAAAGTCTC -3'	<b>APE1 right</b> 5'- GGGGTACGGAGGTCAATTT -3'
<b>Xrcc-5 (Ku80) left</b> 5'- GCGTGAAACCATAGGGAAGA -3'	<b>Xrcc-5 (Ku80) right</b> 5'- CGCCTTCTAAGGACAGCATC -3'
<b>Xrcc6 (Ku70) left</b> 5'- GTCAAGCAAGCTGGAAGACC -3'	<b>Xrcc6 (Ku70) right</b> 5'- GTCAAGCAAGCTGGAAGACC -3'
<b>Lig4 left</b> 5'- ATTCCTGGGACCACTCTCCT -3'	<b>Lig4 right</b> 5'- CTGAATCGGACACCCAACTT -3'
<b>Xrcc1 left</b> 5'- TCTTCTCAAGGCGGACACTT -3'	<b>Xrcc1 right</b> 5'- AGGTCCAAAAATGCGAACAC -3'
<b>Gadd45a left</b> 5'- ATGGCATCCGAATGGAAATA -3'	<b>Gadd45a right</b> 5'- TGAAAGTAACCTGGCCATCC -3'